JOURNAL OF AGRICULTURAL AND FOOD CHEMISTRY

Article

pubs.acs.org/JAFC

# Nontargeted Metabolite Profiling in Compatible Pathogen-Inoculated Tobacco (*Nicotiana tabacum* L. cv. Wisconsin 38) Using UPLC-Q-TOF/MS

Kyoungwon Cho,[†] Yuran Kim,[†] Soo Jin Wi,[†,§] Jong Bok Seo,[†] Joseph Kwon,[‡] Joo Hee Chung,[†] Ky Young Park,[†,§] and Myung Hee Nam*[,†]

[†]Seoul Center, Korea Basic Science Institute (KBSI), Seoul 136-713, Republic of Korea

[§]Department of Biology, Sunchon National University, Sunchon, Chonnam 540-742, Republic of Korea

[‡]Kwangju Center, Korea Basic Science Institute (KBSI), Kwangju 305-806, Republic of Korea

Supporting Information

**ABSTRACT:** A biphasic reactive oxygen species (ROS) production has previously been observed in tobacco at 1 and 48 h after inoculation with the hemibiotrophic compatible pathogen, *Phytophthora parasitica* var. *nicotianae* (*Ppn*). To characterize the response of tobacco to biphasically produced ROS concerning the propagation of *Ppn*, ultraperformance liquid chromatography−quadrupole−time of flight/ mass spectrometry (UPLC-Q-TOF/MS) based metabolic profiling combined with multivariate statistical analysis was performed. Among the nonredundant 355 mass ions in ESI+ mode and 345 mass ions in ESI− mode that were selected as significantly changed by *Ppn* inoculation ($|p(\mathrm{corr})| > 0.6$ on S-plot of orthogonal partial least-squares discriminant analysis (OPLS-DA), fold-change > 2, and $p < 0.05$ in the independent two-sample $t$ test), 76 mass ions were identified on the basis of their accurate mass ions and MS/MS spectra. Phenolic amino acids, phenylpropanoids, hydroxycinnamic acid amides, linoleic acid, linolenic acid, lysophospholipids, glycoglycerolipids, and trioxidized phospholipids were identified as having changed after *Ppn* inoculation. On the basis of their quantitative changes, the metabolic responses occurring at each phase of ROS production after *Ppn* inoculation were investigated in this study.

**KEYWORDS:** *Nicotiana tabacum, metabolomics, UPLC-Q-TOF/MS, ROS, compatible pathogen, phenylpropanoid, HCCAs, lysophospholipid, phytosphingosine*

## INTRODUCTION

Plants are challenged by exposure to a wide range of biotic and abiotic stresses during their lifetime. To withstand the challenges, plants have developed complex and efficient defense mechanisms. These responses include sensing a variety of stresses, activating diverse stress-related signal pathways leading to transcriptional activation of defense responsive gene and altering physiological and metabolic responses.[1−4]

Accumulation of reactive oxygen species (ROS) is a common initial response of plants to biotic and abiotic stresses.[5−9] ROS include superoxide ($O_2^-$), hydrogen peroxide ($H_2O_2$), and lipid peroxides. Lipid peroxides can be converted to oxylipins, which can control segments of cellular signaling pathways. ROS signaling is known to be linked with a variety of signaling networks in plants, including hormonal signaling, mitogen-activated protein kinase (MAPK) cascades, calcium signaling, and homeostasis of cellular redox molecules, such as thioredoxins, perosiredoxins, glutaredoxins, and NADPH.[5−8] However, many challenges remain to understand the relationship between ROS and signaling cascades of plants exposed to stresses.

Typically, a biphasic ROS production, which is a first transient accumulation of ROS and a second prolonged oxidative burst, occurs in incompatible plant−pathogen interactions to activate defense responses, including a hypersensitive response (HR), accumulation of phytoalexins, and expression of pathogenesis-related (PR) genes, as well as to establish enhanced pathogen resistance.[10,11] In contrast, only the first phase of ROS production is observed in compatible interactions. In some cases, a much smaller single-phase ROS burst or no burst at all occurs in plants infected with susceptible pathogens.

Recently, our research group reported a biphasic production of ROS in susceptible tobacco (*Nicotiana tabacum* L. cv. Wisconsin 38) plants after shoot inoculation with *Phytophthora parasitica* var.*nicotianae* (*Ppn*).[12] As compared to the typical pattern of ROS production induced by cryptogein (a HR-inducing elicitor),[6,12−14] the *Ppn* interaction results in a weaker transient accumulation of ROS at 1 h and a delayed second massive burst at 48 h followed by extensive cell death and pathogen proliferation.[12] The effective induction of ROS-detoxifying enzymes and PR proteins is observed only at the second phase of ROS accumulation. Transgenic tobacco with impaired ROS production shows enhanced pathogen resistance, thereby indicating that pathogen tolerance is related to the reduction of ROS.[12] These results imply that the responses followed by the *Ppn*-induced biphasic oxidative burst may differ

Received: August 27, 2012
Revised: October 15, 2012
Accepted: October 16, 2012
Published: October 16, 2012





dx.doi.org/10.1021/jf303702j | J. Agric. Food Chem. 2012, 60, 11015−11028

from an incompatible pathogen−plant interaction that results in a resistance. Thus, we investigated which metabolic response events occurred at the first and second phases of ROS production in *Ppn*-inoculated susceptible tobacco. To investigate the molecular responses, we focused on metabolite profiles.

Metabolomics has emerged as a valuable technology that contributes to the understanding of molecular responses in biological systems.[15] The comprehensive, quantitative, and qualitative measures of cellular metabolites can provide an overview of the biological status of an organism exposed to stress conditions. Currently, many metabolomics studies have been performed to investigate plant responses against environmental stresses.[16−20] Therein, diverse metabolomics approaches have been optimized according to the extraction method, the separation technique, and the detection technique.[21−24] Among these approaches, liquid chromatography (LC) coupled to quadrupole time-of-flight mass spectrometry (Q-TOF/MS)-based metabolome profiling is a versatile tool for metabolite profiling because LC is the most compatible approach with biomolecules, and the enhanced resolution and mass accuracy of Q-TOF MS make the identification of unknown compounds feasible.[25,26] Metabolic information has been subsequently accumulated in several metabolome databases, including the Human Metabolome Database (http://www.hmdb.ca/), METLIN (http://metlin.scripps.edu/), MASS Bank (http://www.massbank.jp/),[27] LIPID MAPS (http://www.lipidmaps.org/),[28] and Respect for Phytochemicals (http://spectra.psc.riken.jp/),[29] which support the identification of profiled metabolites. However, most metabolites are unknown, and the development of an annotation strategy of many unknown peaks is considered to be the most difficult technical challenge.[15,29] MS/MS analysis can be used for deduction of metabolite structure by manual or database-assisted interpretation of the fragmentation pattern of unknown metabolites.

In this study, metabolite profiling using UPLC-Q-TOF/MS was applied to investigate the metabolic responses at the first (1 h) and second (48 h) phases of ROS production occurring in tobacco inoculated with the compatible pathogen, *Ppn*. Pathogen-responsive mass ions were selected using independent sample *t* tests and multivariate statistical analysis, including principal component analysis (PCA) and orthogonal partial least-squares discriminant analysis (OPLS-DA). The selected mass ions were identified by analysis of their MS/MS fragmentation patterns referring to metabolome databases and relevant literature. On the basis of the functions of the identified metabolites, this study investigated the metabolic significance concerning the susceptibility of tobacco to *Ppn*.

## MATERIALS AND METHODS

**Standards and Chemicals.** HPLC grade phenolic compounds such as caffeic acid, *trans*-ferulic acid, and *p*-coumaric acid were obtained from Sigma-Aldrich Korea (Yongin-city, Kyunggi-do, Korea). Lipid standards, including linoleic acid (18:2), linolenic acid (18:3), 1-hexadecanoyl-2-(9*Z*,12*Z*-octadecadienoyl-*sn*-glycero-3-phosphoglycerol [PG (16:0/18:2)], 1-octadecanoyl-*sn*-glycero-3-phosphoethanolamine [LysoPE (18:0)], 1-(9*Z*-octadecenoyl)-*sn*-glycero-3-phosphoethanolamine [LysoPE (18:1)], 1,2-dihexadecanoyl-*sn*-glycero-3-phosphoethanolamine [PE (16:0/16:0)], 1,2-dioctadecanoyl-*sn*-glycero-3-phosphoethanolamine [PE (18:0/18:0)], 1,2-di-(9*Z*,12*Z*-octadecadienoyl)-*sn*-glycero-3-phosphoethanolamine [PE (18:2/18:2)], 1-octadecanoyl-*sn*-glycero-3-phosphocholine [LysoPC (18:0)], 1,2-dihexadecanoyl-*sn*-glycero-phosphocholine [PC (16:0/16:0)], 1,2-dioctadecanoyl-*sn*-glycerophosphocholine [PC (18:0/18:0)], 1,2-di-(9*Z*,12*Z*-octadecadienoyl)-*sn*-glycero-3-phosphocholine [PC (18:2/18:2)], and 1-octadecanoyl-2-(9*Z*,12*Z*-octadecadienoyl)-*sn*-glycero-3-phosphocholine [PC (18:0/18:2)] were purchased from Avanti Polar Lipids, Inc. (USA).

**Plant Material and Pathogen Inoculation.** Seeds of the susceptible tobacco cultivar, *N. tabacum* L. cv. Wisconsin 38, were sterilized in a 0.5% hypochlorite solution and cultured on solid Murashoge and Skoog (MS) medium (pH 5.8) under light (16 h L/8 h D; 50 $\mu$mol photons $m^{-2}$ $s^{-1}$) at room temperature (25 ± 5 °C). *P. parasitica* var. *nicotianae* was maintained on oatmeal agar at 25 °C in the dark. Tobacco shoots with four to five leaves were inoculated directly with a pathogen plug (1 cm in diameter) in a culture bottle containing solid half-strength MS medium as previously described.[12] Plants were then placed in a growth chamber at 25 °C and maintained at 100% relative humidity. As control groups, shoots were incubated in half-strength MS medium without pathogen. The youngest three leaves in each plant at 1 and 48 h post pathogen inoculation (ppi) were collected, immediately frozen in liquid nitrogen, and then stored at −80 °C until metabolite extraction. Eight biological replicates were produced at each time point of treatments.

**Metabolite Extraction.** Frozen samples were ground using a bead beater (4.5 $ms^{-1}$, 25 s, 3 repetitions, MP 24X4, FastPrep-24, MP Biochemical). Subsequently, the ground sample (200 mg) was suspended in methanol with a 0.125% formic acid solution (600 $\mu$L), kept at 4 °C for 30 min, sonicated at 4 °C for 20 s (20 kHz, 250 W, three repetitions, Bioruptor-KRB-01, Bio-Medical Science), and centrifuged at 3000 rpm for 15 min at 4 °C. The supernatant solution was then centrifuged at 13000 rpm for 10 min at 4 °C before UPLC-Q-TOF/MS analysis.

**UPLC-Q-TOF/MS Analysis.** Chromatographic separation was performed on an UPLC system (Waters, Milford, MA, USA) using an Acquity UPLC BEH $C_{18}$ column (2.1 mm × 100 mm, 1.7 $\mu$m, Waters). The mobile phases consisted of solvent A (deionized water/0.1% formic acid) and solvent B (acetonitrile/1% formic acid). The gradient was applied at a flow rate of 0.4 mL/min as follows: solvent B was linearly increased from 3% at 0 min to 50% at 3 min to 70% at 4 min, increased to 100% at 10 min, and held at 100% until 10.5 min. Finally, solvent B was decreased to 3% at 11 min and held at 3% until 12 min. Mass acquisition was performed on a Q-TOF-MS (Synapt HDMS system, Waters, USA) operating in both electrospray ionization (ESI) positive and negative modes with the following parameters: capillary voltage of 2.85 kV for positive and negative modes; cone voltage of 40 V; source temperature of 110 °C; desolvation temperature of 310 °C; and desolvation gas flow of 700 L/h. The mass data were collected in the range of $m/z$ 60−1200 with a scan time of 0.25 s and an interscan time of 0.02 s for 12 min. LC-MS/MS analysis was performed by a collision energy ramp from 20 to 45 eV in the mass range of $m/z$ 60−1200 using automated data-dependent acquisition. To ensure the accuracy of the measured mass, leucine-enkephalin ($m/z$ 556.2771 in positive mode and $m/z$ 554.2771 in negative mode) were used as a reference lock-mass compound at a concentration of 500 pg/$\mu$L and a flow rate of 5 $\mu$L/min.

**Data Processing and Alignment.** In total, 32 LC-MS chromatograms in positive (or negative) mode were obtained from 8 pathogen-inoculated plants and 8 matched controls at each of two time points, 1 and 48 ppi. Peak detection was performed using MarkerLynx software (Waters, USA) with the following parameters: peak intensity threshold of 50 counts and automatic determination of deisotoping, peak width, peak baseline threshold, and noise elimination level. The alignment of mass peaks across all chromatograms was performed using the mass range of $m/z$ 60−1200, mass tolerance of 0.05 Da, retention time window of 0.25 min, and mass window of 0.1 Da. The result was output as a data set containing 4130 and 2136 metabolites represented as retention time and mass-to-charge ratio (RT−$m/z$ pair) in positive and negative modes, respectively.

**Selection of Putative Pathogen-Responsive Metabolites.** The intensities of metabolites for each sample were sum normalized and Pareto scaled using the SIMCA-P+ software package. To compare the metabolite profiles extracted from the pathogen-inoculated

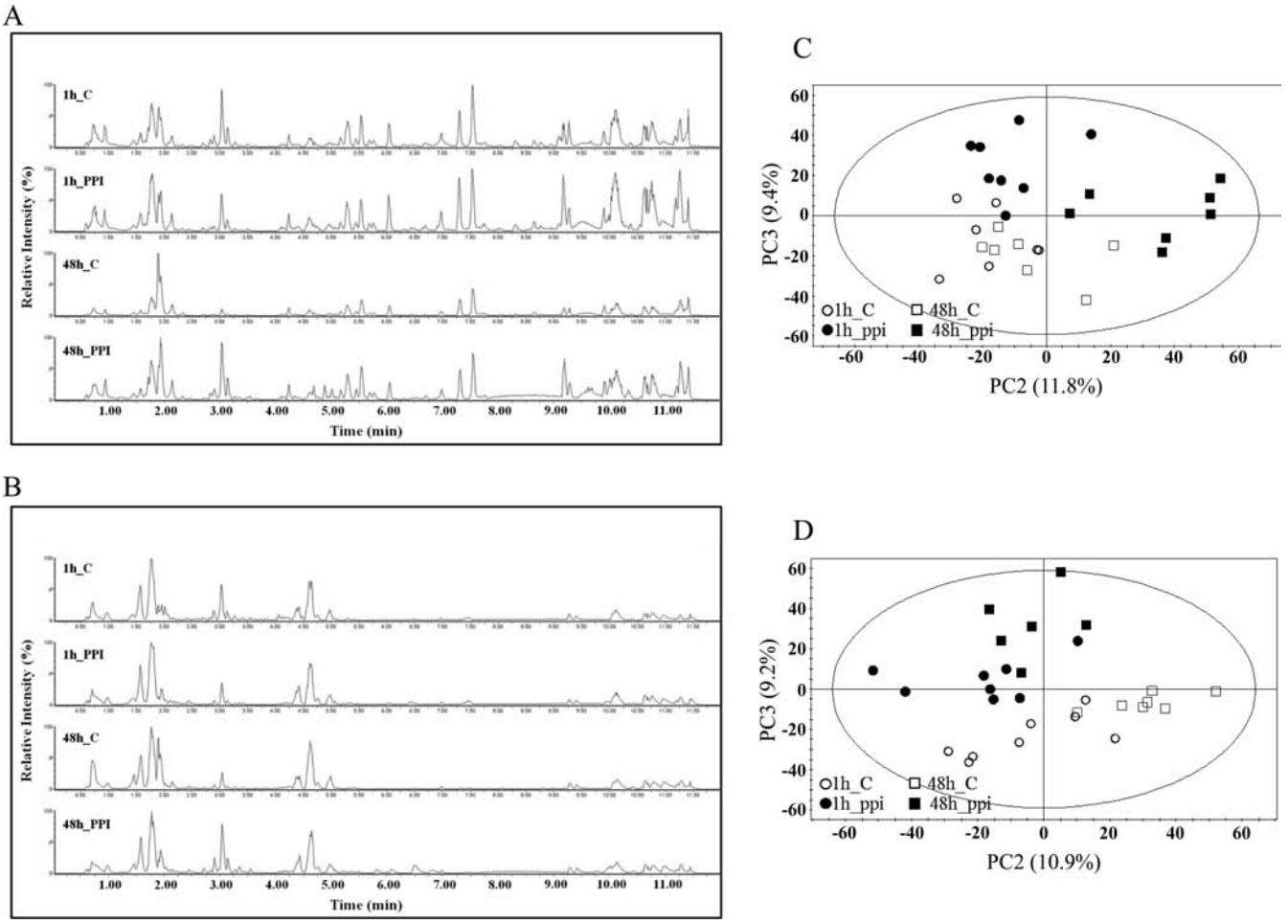


**Figure 1.** Base peak chromatogram and principal component analysis of metabolite profiles extracted from tobacco leaves inoculated with a hemibiotrophic compatible pathogen (*Ppn*). Base peak chromatograms (BCPs) were obtained with TOF mass spectrometers in both positive (A) and negative (B) modes. Principal component analysis of positive (C) and negative (D) metabolite markers obtained from tobacco at 1 and 48 h post compatible pathogen (*Ppn*) inoculation using MarkerLyxn software on peak areas with Pareto scaling. The labels are as follows: 1h_C and 48h_C, control samples harvested at 1 and 48 h, respectively; 1h_PPI and 48h_PPI, samples harvested at 1 and 48 h post compatible pathogen inoculation, respectively.

tobaccos and controls at each time point, we performed two multivariate statistical analysis, PCA and OPLS-DA, with data from 32 samples (4 types of samples × 8 biological replicates) grouped into four classes (1 h ppi, 48 h ppi, 1 h control, and 48 h control). The reliability correlation [$p$(corr)] values of all metabolites from the S-plot of the OPLS-DA was extracted using the first component. We selected metabolites satisfying the following criteria as potential markers: (a) high confidence |$p$(corr)| > 0.6) in discrimination between pathogen-inoculated samples and the corresponding controls at each time point; (b) mean intensities in pathogen-inoculated samples significantly different as compared to those in the controls ($p$ < 0.05); and (c) fold change of two or more in pathogen-inoculated samples as compared to those in the controls. The $p$ value was calculated using independent two-sample $t$ test.

**Metabolite Identification Based on MS/MS Spectra.** For metabolite identification, the following resources were used: molecular formula suggested by the MassLynx software based on the element composition and isotope composition of the parent mass ion; MS/MS spectra of the standard compounds; and metabolome databases, including the Human Metabolomics Database (http://www.hmdb.ca/), METLIN (http://metlin.scripps.edu/), MASS Bank (http://www.massbank.jp/),[27] LIPD MAPS (http://www.lipidmaps.org/),[28] and Respect for Phytochemicals (http://spectra.psc.riken.jp/).[29] In addition, major fragment ions in the MS/MS spectra of potential markers were compared to reports on similar compounds, such as phenolic compounds[30−33] and lipids.[28,34,35] Fragmented or adducted mass features from the parent ion were revealed by comparison of MS/MS spectra of metabolites.

## RESULTS AND DISCUSSION

**Selection of Pathogen-Responsive Mass Ions Based on Statistical Analysis.** The methanol extracts from leaves harvested at 1 and 48 h ppi were analyzed using UPLC-Q-TOF/MS under positive (ESI+) and negative (ESI−) modes resulting in the detection of 4130 and 2136 variables represented as retention time and mass-to-charge ratio (RT−$m/z$ pair) in ESI+ and ESI− modes, respectively. Panels A and B of Figure 1 show the base peak intensity chromatograms of each sample in ESI+ and ESI− modes. To summarize the discrimination among all four groups of samples, 4130 (2136) variables in ESI+ (ESI−) mode were subjected to PCA. Panels C and D of Figure 1 show that 21.2% of the variables in ESI+ mode and 20.1% of the variables in ESI− mode with second and third components were able to distinguish between the pathogen-inoculated groups and control groups.

Furthermore, OPLS-DA was performed to detect discrimination between pathogen-inoculated samples and controls at each time point. The OPLS-DA score plots showed clear

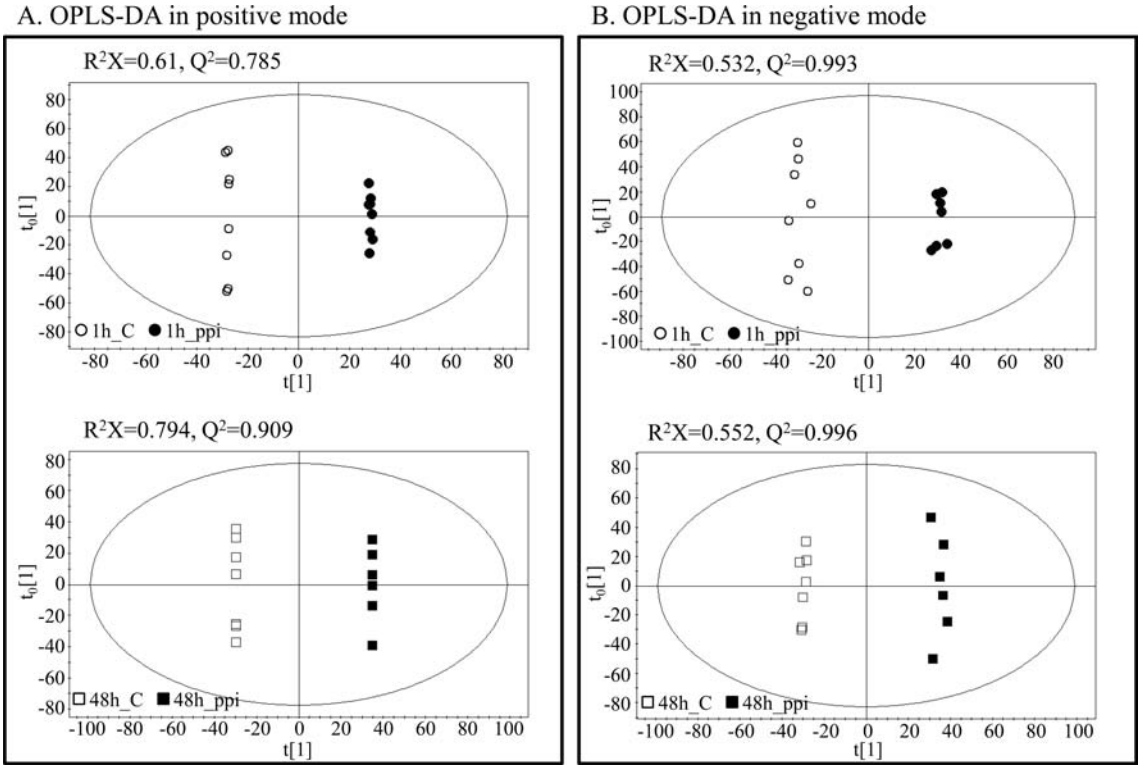


**Figure 2.** Orthogonal partial least-squares discriminant analysis (OPLS-DA). OPLS-DA of positive (C) and negative (D) metabolite markers obtained at 1 and 48 h post compatible pathogen (*Ppn*) inoculation using MarkerLyxn software on peak areas with Pareto scaling. The labels are as follows: 1h_C and 48h_C, control samples harvested at 1 and 48 h, respectively; 1h_ppi and 48h_ppi, samples harvested at 1 and 48 h post compatible pathogen inoculation, respectively.

discrimination between the two groups in ESI+ ($R^2X$ = 0.61 and $Q^2$ = 0.785 at 1 h ppi; and $R^2X$ = 0.61 and $Q^2$ = 0.785 at 48 h ppi) and ESI− ($R^2X$ = 0.532 and $Q^2$ = 0.993 at 1 h ppi; and $R^2X$ = 0.552 and $Q^2$ = 0.996 at 48 h ppi) modes (Figure 2). The following three criteria for selection of pathogen-responsive ions were established: correlation coefficient of ($|p(\mathrm{corr})| > 0.6$ on the S-plot of OPLS-DA; statistical significance of $p < 0.05$ in the independent two-sample $t$ test; and intensity change >2-fold between the two groups releasing 154 pathogen-responsive mass ions at 1 h ppi and 244 at 48 h ppi in ESI+ mode as well as 175 at 1 h ppi and 218 at 48 h ppi in ESI− mode (Supporting Information, Supplementary Tables 1A and 1B). Of the nonredundant 355 (345) mass ions in ESI+ (ESI−) mode, MS/MS spectra of 28 (48) ions were obtained.

**Identification of Pathogen-Responsive Mass Ions Based on MS/MS Spectra.** To identify unknown mass ions selected as changed by *Ppn* inoculation, MS/MS spectra-based identification using metabolome databases, neutral loss, and lipid fragmentation rule was used.

*Identification Based on Metabolome Database.* The mass ions selected with MS/MS spectra were identified using metabolome databases. Fragmentation patterns of mass ions at $m/z$ 120.0786 ($1.44_{RT}$), 146.0589 ($1.70_{RT}$), 188.0685 ($1.71_{RT}$), 177.0537 ($2.08_{RT}$), and 497.2361 ($5.48_{RT}$) in ESI+ mode were similar to those of phenylalanine $[M + H - H_2O - CO]^+$, indole-3-carboxyaldehyde $[M + H]^+$, tryptophan $[M + H - NH_3]^+$, ferulic acid $[M + H - H_2O]^+$, and loroglossin $[M + H - 246]^+$, respectively (Table 1; Supporting Information, Supplementary Figure 1). In ESI− mode, malic acid $[M - H]^-$ at $m/z$ 133.0127 ($0.75_{RT}$), caffeoylquinic acid $[M - H]^-$ at $m/z$ 371.0989 ($1.28_{RT}$), tryptophan $[M - H]^-$ at $m/z$ 203.0813 ($1.70_{RT}$), feruloylquinic acid $[M - H]^-$ at $m/z$ 367.1023 ($2.11_{RT}$), quinic acid $[M - H]^-$ at $m/z$ 191.0547 ($2.16_{RT}$), and a caffeic acid conjugate $[M - H]^-$ at 249.1344 ($2.49_{RT}$) were identified (Table 1; Supporting Information, Supplementary Figure 2).

Moreover, during the MS/MS pattern analysis of the mass ions using metabolome databases, specific daughter ions of a known molecular ion were found to exist within fragment ions of a tested mass ion. For example, $[M + H]^+$ at $m/z$ 314.1365 ($2.88_{RT}$) in ESI+ mode was abundantly fragmented to eight daughter ions with a neutral loss (NL) of 137.07 Da (Figure 3A). Using a metabolome database (http://spectra.psc.riken.jp/), we found that the daughter ions were composed of fragment ions of ferulic acid ($m/z$ 177, 149, 145, 117, and 89) and tyramine with a neutral mass of 137.08 Da ($m/z$ 121, 103, and 77), thereby indicating that $[M + H]^+$ at $m/z$ 314.1365 was a mass ion of the *N*-feruloyltyramine conjugate of ferulic acid and tyramine. This finding indicated that the analysis of neutral loss and specific daughter ions in MS/MS spectra of an unknown molecular ion provides useful information for its identification. Using the same approach, $[M + H]^+$ at $m/z$ 625.2560 ($3.52_{RT}$) fragmented to $m/z$ 488.1437 (NL of 137 Da for one tyramine), and 351.0686 (NL of 274 Da for two tyramines) was identified as a two tyramine-conjugated compound called grossamide (Table 1; Supporting Information, Supplementary Figure 1) for which a similar MS/MS pattern has been observed in the fragmentation of grossamide by positive fast atom bombardment tandem mass spectrometry (FAB-MS/MS).[36] Furthermore, considering a similar retention time and mass difference ($\Delta H_2$) of an identical compound between ESI+ and ESI− modes, feruloyltyramine at $m/z$

**Table 1. Identification of Pathogen-Responsive Mass Ions with MS/MS Spectra Obtained in ESI+ and ESI− Modes**

| RT (min) | adduct[a] | mass ($m/z$) | main fragment ions (relative intensity [fragmented form])[b] | tentative identification | formula | exact mass | Δppm | score[c] |
|---|---|---|---|---|---|---|---|---|
| 0.63[d] | $[M - H]^-$ | 173.1035 | | arginine | $C_6H_{14}N_4O_2$ | 174.1117 | 2.02 | |
| 0.75 | $[M - H]^-$ | 133.0127 | 133.01 (100), 115.00 (15.5 $[M - H_2O - H]^-$), 111.00 (12.1) | malic acid | $C_4H_6O_5$ | 134.0215 | 7.52 | 0.999 |
| 1.13[d] | $[M - H]^-$ | 180.0658 | | tyrosine | $C_9H_{11}NO_3$ | 181.0739 | 1.49 | |
| 1.28 | $[M - H]^-$ | 371.0989 | 191.05 (100), 135.04 (19) | caffeoylquinic acid | $C_{16}H_{18}O_9$ | 354.0950 | 3.37 | 0.694 |
| 1.44 | $[M + H - CH_2O_2]^+$ | 120.0786 | 120.07 (41), 103.05 (100), 91.05 (24), 77.03 (44) | phenylalanine | $C_9H_{11}NO_2$ | 165.0790 | 17.58 | 0.930 |
| 1.44[d] | $[M - H]^-$ | 164.0712 | | phenylalanine | $C_9H_{11}NO_2$ | 165.0790 | 0.28 | |
| 1.45[d] | $[M + H]^+$ | 166.0857 | | phenylalanine | $C_9H_{11}NO_2$ | 165.0790 | 6.69 | |
| 1.70 | $[M + H]^+$ | 146.0589 | 118.06 (100), 117.05 (77), 91.05 (73) | indole-3-carboxyaldehyde | $C_9H_7NO$ | 145.0528 | 13.10 | 0.948 |
| 1.70[d] | $[M - H]^-$ | 159.0918 | | tryptamine | $C_{10}H_{12}N_2$ | 160.1000 | 2.64 | |
| 1.70 | $[M - H]^-$ | 203.0813 | 203.07 (3.5), 142.06 (12.8), 116.05 (100) | tryptophan | $C_{11}H_{12}N_2O_2$ | 204.0899 | 2.85 | 0.687 |
| 1.71 | $[M + H - NH_3]^+$ | 188.0695 | 170.05 (11), 146.05 (17), 143.06 (82), 118.06 (100), 115.05 (87), 91.05 (31) | tryptophan | $C_{11}H_{12}N_2O_2$ | 204.0899 | 13.73 | 0.731 |
| 2.08 | $[M + H - H_2O]^+$ | 177.0537 | 149.06 (50), 134.03 (43), 117.03 (100), 89.03 (71) | ferulic acid | $C_{10}H_{10}O_4$ | 194.0579 | 8.25 | 0.730 |
| 2.11 | $[M - H]^-$ | 367.1023 | 193.05 (12.9), 191.05 (100), 173.04 (18.6), 134.03 (31.7), 93.03 (15.7) | feruloylquinic acid | $C_{17}H_{20}O_9$ | 368.1107 | 1.18 | 0.886 |
| 2.16 | $[M - H]^-$ | 191.0547 | 191.05 (100), 109.02 (33.3), 85.03 (26.7) | quinic acid | $C_7H_{12}O_6$ | 192.0634 | 3.61 | 0.987 |
| 2.49 | − | 249.1344 | 249.12 (24.8), 207.10 (12.8), 135.04 (100) | unknown | | | | |
| 2.73 | − | 821.3249 | 821.30 (17.7), 698.24 (79.0), 666.21 (100), 638.23 (10.0), 257.13 (6.0) | unknown | | | | |
| 2.75 | − | 561.2216 | 561.31 (63.6), 503.31 (100), 457.18 (54.5) | unknown | | | | |
| 2.87 | − | 585.2919 | 543.26 (100) | unknown | | | | |
| 2.87 | + | 714.2897 | 714.25 (21), 682.22 (100), 650.20 (12), 520.18 (22), 488.16 (32), 460.16 (19), 367.11 (28) | hexose- or caffeoyl-conjugated compound | | | | |
| 2.88 | $[M + H]^+$ | 314.1365 | 177.04 (71), 149.05 (13), 145.02 (100), 121.06 (51), 117.03 (82), 103.05 (14), 89.03 (61), 77.03 (6) | feruloyltyramine | $C_{18}H_{19}NO_4$ | 313.1314 | 9.58 | |
| 2.88 | + | 805.3345 | 805.28 (38), 773.26 (27), 684.24 (31), 643.24 (36), 611.21 (50), 522.20 (100), 490.17 (17), 458.14 (20), 357.12 (13), 337.10 (18),325.10 (9), 204.05 (9), 166.07 (3) | hexose- or caffeoyl-conjugated compound | | | | |
| 2.89 | − | 835.3405 | 835.11 (59.0), 803.29 (100), 771.26 (73.3), 666.20 (76.9) | unknown | | | | |
| 2.90 | $[M - H]^-$ | 312.1227 | 312.11 (21.0), 190.05 (95.2), 178.04 (93.5), 148.05 (100), 135.04 (66.1) | feruloyltyramine[e] | $C_{18}H_{19}NO_4$ | 313.1314 | 9.58 | |
| 2.98 | − | 921.3427 | 877.32 (86.9), 845.30 (100.0), 813.27 (67.3), 708.21 (38.3) | unknown | | | | |
| 3.00 | + | 645.2932 | 645.28 (46), 613.23 (100), 595.21 (54), 522.19 (23), 490.17 (58), 449.16 (81), 337.11 (73), 325.10 (42), 204.05 (27), 166.07 (15) | fragment ion of $m/z$ 807.3491 | | | | |
| 3.01 | + | 807.3491 | 807.31 (58), 775.28 (100), 684.24 (20), 652.21 (21), 645.25 (24), 613.23 (88), 522.19 (7), 490.17 (21), 449.16 (22), 337.10 (24), 325.10 (9), 204.05 (14), 166.07 (5) | hexose- or caffeoyl-conjugated compound | | | | |
| 3.03 | − | 805.3303 | 805.30 (72.8), 773.28 (100.0), 651.22 (37.7) | unknown | | | | |
| 3.12 | + | 893.3543 | 893.30 (90), 861.27 (77), 770.24(26), 739.23 (15), 645.26 (11), 613.23 (100), 490.15 (30), 448.16 (27), 337.10 (18), 204.05 (8), 166.07 (2) | malonylhexose-conjugated compound | | | | |
| 3.13 | − | 847.3390 | 847.32 (92.3), 815.29 (100.0), 693.24 (35.9), 648.24 (6.2) | unknown | | | | |
| 3.13 | − | 891.3327 | 891.30 (0.9), 847.31 (92.3), 815.29 (100.0), 693.24 (32.2), 490.19 (2.7) | unknown | | | | |
| 3.14 | − | 315.0510 | 300.02 (92.0), 271.03 (100.0), 255.02 (44.0) | unknown | | | | |
| 3.15 | − | 1139.6080 | 569.30 (3.1), 525.30 (100.0), 465.27 (10.8) | unknown | | | | |
| 3.30 | $[M - H]^-$ | 547.3491 | 487.31 (100.0 $[M - H - 60]^-$), 343.28 (90.0 $[M - H - 60 - 163]^-$) | tyramine conjugated compound | | | | |
| 3.52 | $[M + H]^+$ | 625.2560 | 625.22 (21), 488.14 (19), 462.17 (37), 351.07 (100), 325.09 (95), 307.08 (68), 293.07 (40), 265.07 (23), 201.04 (13), 121.06 (10) | grossamide[f] | $C_{36}H_{36}N_2O_8$ | 624.2472 | 1.28 | |
| 3.55 | $[M - H]^-$ | 623.2374 | 623.22 (59.9), 460.17 (100.0 $[M - H - 163]^-$), 432.16 (37.1), 297.11 (66.5 $[M - H - 163 - 163]^-$), 283.09 (19.8) | grossamide | $C_{36}H_{36}N_2O_8$ | 624.2472 | 2.89 | |
| 3.88 | + | 535.2922 | 535.25 (83), 449.29 (100) | unknown | | | | |
| 4.02 | $[M + FA - H]^-$ | 659.3649 | 659.32 (3.4), 613.33 (100.0) | unknown | | | | |



dx.doi.org/10.1021/jf303702j | J. Agric. Food Chem. 2012, 60, 11015−11028

**Table 1. continued**

| RT (min) | adduct[a] | mass ($m/z$) | main fragment ions (relative intensity [fragmented form])[b] | tentative identification | formula | exact mass | Δppm | score[c] |
|---|---|---|---|---|---|---|---|---|
| 4.04 | + | 269.2264 | 269.20 (57), 199.13 (43), 185.12 (50), 171.10 (71), 157.09 (100), 143.07 (100), 128.05 (93), 119.08 (50), 105.07 (43), 91.05 (50) | unknown | | | | |
| 4.09 | + | 1091.1110 | 1091.29 (100), 833.91 (52), 783.39 (23), 733.85 (39), 684.31 (27), 627.79 (34), 571.24 (20) | unknown | | | | |
| 4.13 | − | 653.3111 | 653.34 (24.5), 611.32 (100.0), 247.07 (45.1), 101.02 (53.9) | unknown | | | | |
| 4.45 | + | 1032.3440 | 1032.54 (98), 878.95 (65), 776.90 (56), 720.35 (39), 586.33 (100) | unknown | | | | |
| 4.58 | $[M + H]^+$ | 318.2996 | 318.28 (14), 300.28 (21), 282.26 (100), 264.26 (36) | phytosphingosine | $C_{18}H_{39}NO_3$ | 317.2930 | 4.42 | |
| 4.62 | + | 335.2570 | 336.24 (100) | unknown | | | | |
| 4.66 | $[M - H]^-$ | 593.2735 | 593.25 (100.0 $[M - H]^-$), 277.21 (59.9 $[LnA - H]^-$), 241.01 (19.8 $[PI - H_2O - H]^-$), 152.99 (43.0 $[GP - H_2O - H]^-$) | LysoPI (18:3) | $C_{27}H_{47}O_{12}P$ | 594.2805 | 1.65 | |
| 4.67 | $[M + H]^+$ | 518.3246 | 518.29 (3), 184.06 (100), 124.99 (18), 86.09 (19) | LysoPC (18:3) | $C_{26}H_{48}NO_7P$ | 517.3168 | 0.39 | |
| 4.70 | $[M + FA - H]^-$ | 562.3159 | 502.28 (18.0 $[M + FA - 60 - H]^-$), 277.21 (100.0 $[LnA - H]^-$) | LysoPC (18:3) | $C_{26}H_{48}NO_7P$ | 517.3168 | 2.80 | |
| 4.74 | $[M + FA - H]^-$ | 721.2969 | 675.34 (17.4 $[M - H]^-$), 415.14 (52.9 $[M - (LnA - H_2O) - H]^-$), 397.12 (100.0 $[M - (LnA - H_2O) - H_2O - H]^-$), 277.21 (85.1 $[LnA - H]^-$) | DGMG (18:3) | $C_{33}H_{56}O_{14}$ | 676.3670 | 29.72 | |
| 4.89[d] | $[M - H]^-$ | 293.2100 | | hydroxylinolenic acid | $C_{18}H_{30}O_3$ | 294.2195 | 5.68 | |
| 5.00 | $[M + H]^+$ | 520.3406 | 520.31 (3), 184.06 (100), 124.99 (18), 86.09 (19) | LysoPC (18:2) | $C_{26}H_{50}NO_7P$ | 519.3325 | 0.19 | |
| 5.01 | $[M + FA - 60 - H]^-$ | 504.3081 | 279.22 (100.0 $[LA - H]^-$) | LysoPC (18:2) | $C_{26}H_{50}NO_7P$ | 519.3325 | 1.78 | |
| 5.01 | $[M + FA - H]^-$ | 564.3298 | 504.30 (30 $[M + FA - 60 - H]^-$), 279.22 (100.0 $[LA - H]^-$) | LysoPC (18:2) | $C_{26}H_{50}NO_7P$ | 519.3325 | 0.30 | |
| 5.11[d] | $[M - H]^-$ | 291.1979 | | ketolinolenic acid | $C_{18}H_{28}O_3$ | 292.2038 | 6.43 | |
| 5.12 | $[M - H]^-$ | 595.2871 | 595.28 (80.3 $[M - H]^-$), 279.23 (100.0 $[LA - H]^-$), 241.00 (27.6 $[PI - H_2O - H]^-$), 152.99 (40.8 $[GP - H_2O - H]^-$) | LysoPI (18:2) | $C_{27}H_{49}O_{12}P$ | 596.2961 | 1.79 | |
| 5.21 | $[M - H]^-$ | 653.3743 | 415.13 (24.6 $[M - (PA - H_2O) - H]^-$), 397.12 (55.7 $[M - (PA - H_2O) - H_2O - H]^-$), 255.23 (100.0 $[PA - H]^-$) | DGMG (16:0) | $C_{31}H_{58}O_{14}$ | 654.3827 | 0.55 | |
| 5.21 | $[M + FA - H]^-$ | 699.3785 | 653.37 (22.6 $[M - H]^-$), 415.17 (16.1 $[M - (PA - H_2O) - H]^-$), 397.12 (38.7 $[M - (PA - H_2O) - H_2O - H]^-$), 255.23 (100.0 $[PA - H]^-$) | DGMG (16:0) | $C_{31}H_{58}O_{14}$ | 654.3827 | 0.55 | |
| 5.11[d] | $[M - H]^-$ | 295.2268 | | hydroxylinoleic acid | $C_{18}H_{32}O_3$ | 269.2351 | 3.73 | |
| 5.27 | $[M - H]^-$ | 431.2206 | 277.19 (3.6 $[LnA - H]^-$), 152.99 (100.0 $[GP - H_2O - H]^-$), 78.96 (33.9 $[PO_3]^-$) | LysoPA (18:3) | $C_{21}H_{37}O_7P$ | 432.2276 | 2.10 | |
| 5.27 | $[M - H]^-$ | 664.4158 | 664.40 (100.0) | unknown | | | | |
| 5.45 | $[M - H]^-$ | 452.2784 | 255.23 (100.0 $[PA - H]^-$), 196.04 (6.3 $[GPE - H_2O - H]^-$), 78.96 (6.3 $[PO_3]^-$) | LysoPE (16:0) | $C_{21}H_{44}NO_7P$ | 453.2855 | 1.90 | |
| 5.48 | $[M + H - 246]^+$ | 497.2361 | 497.20 (100), 395.14 (38) | loroglossin | $C_{34}H_{46}O_{18}$ | 742.2684 | 16.85 | 0.981 |
| 5.50 | + | 457.2435 | 169.04 (12), 127.03 (100), 109.02 (32), 97.02 (11), 81.03 (25) | unknown | | | | |
| 5.69 | $[M - H]^-$ | 445.2364 | 277.21 (100.0 $[LnA - H]^-$) | linolenic acid conjugated lipid | | | | |
| 5.88 | $[M - H]^-$ | 433.2352 | 279.23 (6.5 $[LA - H]^-$), 152.99 (100.0 $[GP - H_2O - H]^-$), 78.96 (29.0 $[PO_3]^-$) | LysoPA (18:2) | $C_{21}H_{39}O_7P$ | 434.2433 | 0.33 | |
| 5.94 | $[M - H]^-$ | 481.2568 | 253.20 (12.7 $[PLA - H]^-$), 245.04 (100.0 $[GPG - H]^-$), 170.99 (12.7 $[GP - H]^-$), 152.99 (57.9 $[GP - -H_2O - H]^-$), 78.96 (18.3 $[PO_3]^-$) | LysoPG (16:1) | $C_{22}H_{43}O_9P$ | 482.2645 | 0.62 | |
| 6.15 | $[M - H]^-$ | 555.2840 | 555.27 (100.0 $[M - H]^-$), 255.23 (2.5 $[PA - H]^-$) | LysoPI (P-16:0) | $C_{25}H_{49}O_{11}P$ | 556.3012 | 16.66 | |
| 6.31 | $[M - H]^-$ | 483.2720 | 483.26 (6.8 $[M - H]^-$), 255.23 (100.0 $[PA - H]^-$), 152.99 (6.4 $[GP - H_2O - H]^-$) | LysoPG (16:0) | $C_{22}H_{45}O_9P$ | 484.2801 | 0.25 | |
| 6.56 | $[M - H]^-$ | 447.2508 | 279.22 (100.0 $[LA - H]^-$) | linoleic acid conjugated lipid | | | | |
| 6.65 | + | 599.4121 | 599.37 (100), 507.21 (62) | unknown | | | | |
| 6.87[d] | $[M - H]^-$ | 277.2175 | | linolenic acid | $C_{18}H_{30}O_2$ | 278.2246 | 2.68 | |
| 7.02 | $[M + FA - H]^-$ | 746.4747 | 746.49 (100 $[M + FA - H]^-$), 279.22 (100 $[LA - H]^-$), 199.12 (40 $[(oxo\text{-}11:0) - H]^-$) | PC (oxo-11:0/18:2) | $C_{37}H_{68}NO_9P$ | 701.4632 | 18.59 | |
| 7.25 | $[M + H]^+$ | 826.5286 | 826.78 (100), 794.45 (2), 184.06 (86), 124.99 (10), 86.09 (13) | PC (18:3/18:3 + $O_3$) | $C_{44}H_{76}NO_{11}P$ | 825.5156 | 6.05 | |
| 7.28 | $[M + FA - H]^-$ | 870.5166 | 824.47 (17.3 $[M - H]^-$), 810.48 (100.0 $[M + FA - 60 - H]^-$), 325.19 (45.7 $[LnA + O_3 - H]^-$), 293.18 (21.0 $[LnA + O - H]^-$), 277.20 (19.8 $[LnA - H]^-$), 249.17 (4.9 $[LnA + O - CO_2 - H]^-$) | PC (18:3/18:3 + $O_3$) | $C_{44}H_{76}NO_{11}P$ | 825.5156 | 4.04 | |



dx.doi.org/10.1021/jf303702j | J. Agric. Food Chem. 2012, 60, 11015−11028

**Table 1. continued**

| RT (min) | adduct[a] | mass ($m/z$) | main fragment ions (relative intensity [fragmented form])[b] | tentative identification | formula | exact mass | Δppm | score[c] |
|---|---|---|---|---|---|---|---|---|
| 7.30 | $[M - H]^-$ | 782.4615 | 782.44 (100.0 $[M - H]^-$), 474.26 (7.4 [M-(LnA + $O_3$ − $H_2O$) − $H]^-$), 325.20 (76.5 [LnA + $O_3$ − $H]^-$), 293.17 (77.8 [LnA + O − $H]^-$), 277.21 (68.7 [LnA − $H]^-$), 249.18 (18.5 [LnA + O − $CO_2$ − $H]^-$) | PE (18:3/18:3 + $O_3$) | $C_{41}H_{70}NO_{11}P$ | 783.4868 | 1.08 | |
| 7.66[d] | $[M - H]^-$ | 279.2314 | | linoleic acid | $C_{18}H_{32}O_2$ | 280.2402 | 3.58 | |
| 7.79 | $[M - H]^-$ | 634.4088 | 634.40 (40.2 $[M - H]^-$), 452.28 (7.7 [M − (oxo-11:0) − $H_2O$ − $H]^-$), 255.23 (59.8 [PA − $H]^-$), 199.13 (100.0 [(oxo-11:0) − $H]^-$) | PE (oxo-11:0/16:0) | $C_{32}H_{62}NO_9P$ | 635.4162 | 0.64 | |
| 7.80 | + | 589.2474 | 589.21 (100), 529.20 (18), 485.20 (16) | unknown | | | | |
| 8.00 | $[M + FA - H]^-$ | 872.5290 | 872.50 (17.0 [M + FA − $H]^-$), 826.50 (15.2 $[M - H]^-$), 812.50 (100.0 [M + FA − 60 − $H]^-$), 504.31 (2.7 [M − (LnA + $O_3$ − $H_2O$) − $H]^-$), 339.21 (7.1 [LnA + O + FA − $H]^-$), 325.20 (21.4 [LnA + $O_3$ − $H]^-$), 293.17 (21.4 [LnA + O − $H]^-$), 279.23 (22.3 [LA − $H]^-$) | PC (18:2/18:3 + $O_3$) | $C_{44}H_{78}NO_{11}P$ | 827.5312 | 0.30 | |
| 8.67 | $[M - H]^-$ | 1069.6010 | 1069.59 (100.0 $[M - H]^-$), 837.37 (7.1 [M − (HTA − $H_2O$) − $H]^-$), 819.38 (31.4 [M − (HTA − $2H_2O$) − $H]^-$), 791.34 (32.9 [M − (LnA − $2H_2O$) − $H]^-$), 577.18 (20.0 [M − (LnA + HTA − $2H_2O$) − $H]^-$), 559.17 (85.7 [M − (LnA + HTA − $2H_2O$) − $H_2O$ − $H]^-$), 541.16 (67.1 [M − (LnA + HTA − $2H_2O$) − $2H_2O$ − $H]^-$), 397.12 (5.7 [M − (LnA + HTA − $2H_2O$) − $H_2O$ − Hex − $H]^-$), 277.21 (8.6 [LnA − $H]^-$), 249.17 (7.1 [HTA − $H]^-$) | TGDG (16:3/18:3) | $C_{55}H_{90}O_{20}$ | 1070.6026 | 6.03 | |
| 8.67 | $[M + FA - H]^-$ | 1115.6080 | 1115.59 (1.6 [M + FA − $H]^-$), 1069.6 (100.0 $[M - H]^-$), 837.38 (11.7 [M − (HTA − $H_2O$) − $H]^-$), 819.38 (25.9 [M − (HTA − $2H_2O$) − $H]^-$), 809.36 (13.4 [M − (LnA − $H_2O$) − $H]^-$), 791.35 (27.8 [M − (LnA − $2H_2O$) − $H]^-$), 577.18 (7.0 [M − (LnA + HTA − $2H_2O$) − $H]^-$), 559.17 (44.0 [M − (LnA + HTA − $2H_2O$) − $H_2O$ − $H]^-$), 541.15 (41.2 [M − (LnA + HTA − $2H_2O$) − $2H_2O$ − $H]^-$), 397.12 (3.7 [M − (LnA + HTA − $2H_2O$) − $H_2O$Hex − $H]^-$), 277.22 (2.7 [LnA − $H]^-$), 249.18 (2.7 [HTA − $H]^-$) | TGDG (16:3/18:3) | $C_{55}H_{90}O_{20}$ | 1070.6026 | 7.35 | |
| 8.71 | $[M + H]^+$ | 804.5444 | 804.50 (100), 184.06 (53), 124.99 (6), 86.09 (7) | PC (16:0/18:3 + $O_3$) | $C_{42}H_{78}NO_{11}P$ | 803.5313 | 6.22 | |
| 8.75 | $[M + FA - H]^-$ | 848.5261 | 848.48 (11.7 [M + FA − $H]^-$), 802.53 (20.0 $[M - H]^-$), 788.49 (100.0 [M + FA − 60 − $H]^-$), 480.31 (6.9 [M − (LnA + $O_3$) − $H]^-$), 325.19 (27.6 [LnA + $O_3$ − $H]^-$), 293.17 (20.7 [LnA + O − $H]^-$), 255.23 (15.9 [PA − $H]^-$) | PC (16:0/18:3+ $O_3$) | $C_{42}H_{78}NO_{11}P$ | 803.5313 | 3.10 | |
| 8.80 | $[M - H]^-$ | 760.4773 | 60.45 (100.0 $[M - H]^-$) 452.29 (9.2 [M − (LnA + $O_3$ − $H_2O$) − $H]^-$), 325.19 (60.0 [LnA + $O_3$ − $H]^-$), 293.17 (49.2 [LnA + O − $H]^-$), 255.22 (42.3 [PA − $H]^-$), 249.19 (10.0 [LnA + O − $CO_2$ − $H]^-$) | PE (16:0/18:3 + $O_3$) | $C_{39}H_{72}NO_{11}P$ | 761.4843 | 1.31 | |
| 8.89 | + | 655.4014 | 655.36 (100), 597.32 (35), 539.29 (30) | unknown | | | | |
| 9.23 | $[M - H]^+$ | 503.1093 | 503.08 (1), 415.01 (16), 398.99 (2), 341.00 (11), 326.95 (50), 281.03 (100), 265.01 (29), 221.07 (14), 207.02 (4), 147.06 (34),73.04 (13) | dimer of sulfamethoxazole[g] | $C_{20}H_{20}N_6O_6S_2$ | 504.0886 | 57.54 | |
| 9.30 | + | 607.2934 | 607.23 (100), 547.23 (57), 461.20 (14) | unknown | | | | |
| 9.89 | $[M + FA - H]^-$ | 797.5392 | 797.50 (4.9 [M + FA − $H]^-$), 751.52 (3.8 $[M - H]^-$), 491.31 (3.1 [M − (LnA − $H_2O$) − $H]^-$), 277.21 (81.3 [LnA − $H]^-$), 255.23 (100.0 [PA − $H]^-$), 253.08 (4.2 [M − (LnA − $H_2O$) − (PA − $H_2O$) − $H]^-$) | MGDG (16:0/18:3) | $C_{43}H_{76}O_{10}$ | 752.5439 | 2.67 | |

[a] +, ESI+ mode; −, ESI− mode. [b] Abbreviations: FA, formic acid; PA, palmitic acid (16:0); PLA, palmitoleic acid (16:1); LA, linoleic acid (18:2); LnA, linolenic acid (18:3); LnA + $O_3$, trioxidized linolenic acid (18:3 + $O_3$); oxo-(11:0), oxoundecanoic acid; Hex, hexose; HTA, hexadecatrienoic acid (16:3); LysoPA, lysophosphatidic acid; (Lyso)PC, (lyso)phosphatidylcholine; (Lyso)PE, (lyso)phosphatidylethanolamine; LysoPG, lysophosphatidylglycerol; LysoPI, lysophosphatidylinositol; DGMG, digalactosylmonoacylglycerol lipid; MGDG, monogalactosyldiacylglycerol lipid; TGDG, trigalactosyldiacylglycerol lipid. [c] Score is defined as similarity between MS/MS spectra of an observed mass ion and those of a compound opened in web metabolome database (http://spectra.psc.riken.jp/). [d] Identification based on accurate mass value and retention time of standantds: +, ESI+ mode; −, ESI− mode. [e] Reference 37 [f] Reference 36. [g] Reference 38.



dx.doi.org/10.1021/jf303702j | J. Agric. Food Chem. 2012, 60, 11015−11028

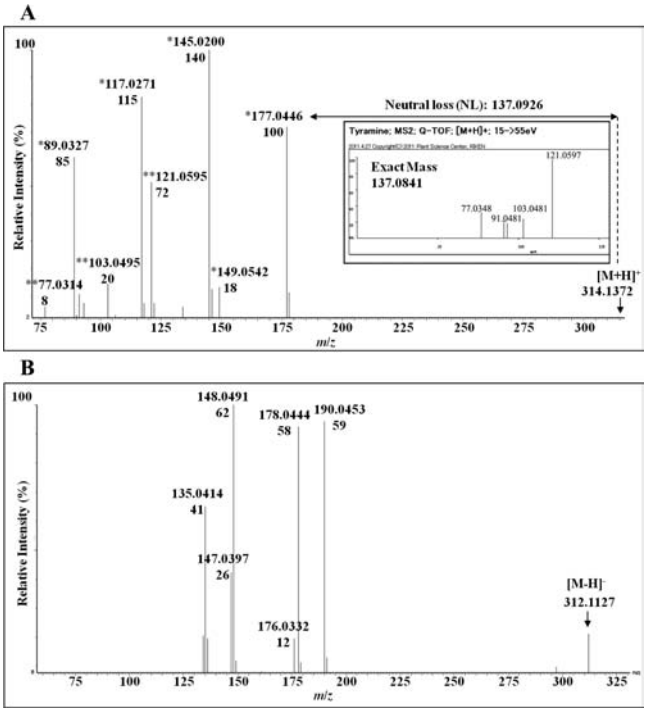


**Figure 3.** Analysis of MS/MS fragmentation of feruloyltyramine in both positive (A) and negative (B) modes. Panel A shows the MS/MS spectra of feruloyltyramine ($m/z$ 314.1365) in positive mode; inner spectra are MS/MS spectra of tyramine recorded in the metabolome database of Respect for Phytochemicals (http://spectra.psc.riken.jp). * represents ferulic acid fragment ions, ** represents tyramine fragment ions, and NL represents neutral loss. Panel B shows the MS/MS spectra of feruloyltyramine ($m/z$ 312.1227) in negative mode.

314.1365 ($2.88_{RT}$) and grossamide at $m/z$ 625.2560 ($3.52_{RT}$) in ESI+ mode were identical with molecules at $m/z$ 312.1227 ($2.90_{RT}$) and 623.2374 ($3.55_{RT}$), respectively. Moreover, the MS/MS spectra of feruloyltyramine in ESI− (Figure 3B) were observed to be similar to those of feruloyltyramine derived from HPLC-MS analysis in tobacco.[37] In addition, the MS/MS spectra of $[M + H]^+$ at $m/z$ 503.1093 ($9.23_{RT}$) were observed to be similarly matched with the GC-MS spectrum of a sulfamethoxazole dimer.[38]

*Identification Based on Analysis of Neutral Loss.* In ESI+ mode, the MS/MS patterns of mass ions at $m/z$ 714.2897 ($2.87_{RT}$), 805.3345 ($2.88_{RT}$), 807.3491 ($3.01_{RT}$), and 893.3543 ($3.12_{RT}$) contained a neutral loss of 162 Da for hexose or caffeoyl group and 248 Da for malonylhexose,[32] thereby indicating that these molecules were hexose- (or caffeoyl-) and malonylhexose-conjugated compounds (Table 1; Supporting Information, Supplementary Figure 1). Furthermore, the MS/MS spectra of mass ions at $m/z$ 645.2473 ($3.00_{RT}$) and 807.3491 ($3.01_{RT}$) showed similar MS fragmentation patterns and retention times, thereby indicating that an ion at $m/z$ 645.2473 was most likely a fragment ion of $m/z$ 807.3491 with a neutral loss of 162 Da (hexose or caffeoyl moiety). The fragment ions derived from a parent ion are generally detected in a number of mass ions produced by MS techniques.

In ESI− mode, the precursor ions of $m/z$ 805.3303 ($3.03_{RT}$), 847.3390 ($3.13_{RT}$), and 891.3327 ($3.13_{RT}$) showed common neutral losses (NL) of 32 and 122 Da (Table 1; Supporting Information, Supplementary Figure 2). The fragmentation patterns of the following three ions indicated that the three compounds have the same moiety (NL of 122 Da): ion at $m/z$ 805.3303 was fragmented to $m/z$ 773.2775 (NL: 32) and 651.2224 (NL: 32 + 122); ion at $m/z$ 847.3390 was fragmented

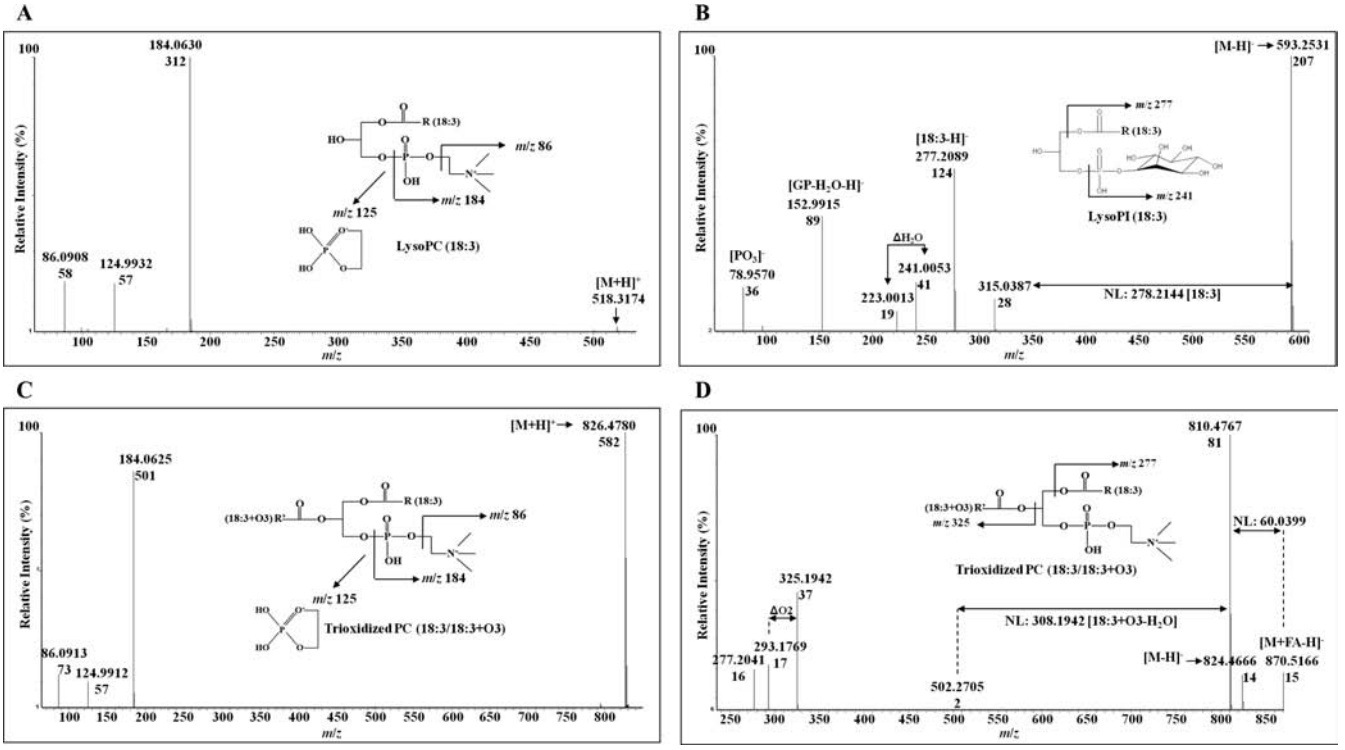


**Figure 4.** Analysis of MS/MS fragmentation of phospholipids. (A) MS/MS spectra of LysoPC (18:3) in positive mode; (B) MS/MS spectra of LysoPI (18:3) in negative mode; (C) MS/MS spectra of trioxidized PC (18:3/18:3 + $O_3$) in positive mode; (D) MS/MS spectra of trioxidized PC (18:3/18:3 + $O_3$) in negative mode.

**Table 2. Relative Levels of *Ppn*-Responsive Metabolites Accumulated at Early Oxidative Burst (1 h ppi) and Second Burst (48 h ppi)**

| | | | | | 1 h ppi | | 48 h ppi | |
|---|---|---|---|---|---|---|---|---|
| FC | RT (min) | mass ($m/z$) | adduct | tentative identification | $\log_2$[a] | $p$ value[b] | $\log_2$ | $p$ value |
| 1. carbohydrates | | | | | | | | |
| | 0.75 | 133.0127 | $[M - H]^-$ | malic acid | 1.07 | 0.0003 | −0.12 | 0.6807 |
| | 2.16 | 191.0547 | $[M - H]^-$ | quinic acid | 1.66 | 0.0082 | 0.07 | 0.8909 |
| 2. amino acids | | | | | | | | |
| | 0.63[c] | 173.103 | $[M - H]^-$ | arginine | 1.18 | 0.0097 | −0.71 | 0.0604 |
| | 1.13[c] | 180.065 | $[M - H]^-$ | tyrosine | −0.68 | 0.2305 | 1.75 | 0.0239 |
| | 1.44 | 120.0786 | $[M + H - CH_2O_2]^+$ | phenylalanine | −0.70 | 0.0481 | 1.56 | 0.0115 |
| | 1.44[c] | 164.0712 | $[M - H]^-$ | phenylalanine | −0.66 | 0.1008 | 1.92 | 0.0294 |
| | 1.45[c] | 166.0857 | $[M + H]^+$ | phenylalanine | −0.77 | 0.0252 | 1.35 | 0.0395 |
| | 1.70 | 203.0813 | $[M - H]^-$ | tryptophan | −1.09 | 0.0866 | 1.51 | 0.0300 |
| | 1.71 | 188.0695 | $[M + H - NH_3]^+$ | tryptophan | −0.88 | 0.0860 | 1.42 | 0.0038 |
| 3. secondary metabolites (phenolic compounds) | | | | | | | | |
| | 1.28 | 371.0989 | $[M + H_2O - H]^-$ | caffeoylquinic acid | −1.14 | 0.0021 | −0.71 | 0.0420 |
| | 1.70 | 146.0589 | $[M - H]^-$ | indole-3-carboxyaldehyde | −0.80 | 0.1184 | 1.42 | 0.0052 |
| | 1.70[c] | 159.0918 | $[M - H]^-$ | tryptamine | −0.99 | 0.0973 | 1.53 | 0.0280 |
| | 2.08 | 177.0537 | $[M + H - H_2O]^+$ | ferulic acid | 1.28 | 0.0085 | −0.38 | 0.2498 |
| | 2.11 | 367.1023 | $[M - H]^-$ | feruloylquinic acid | 1.65 | 0.0024 | −0.01 | 0.9674 |
| | 2.49 | 249.1344 | | caffeic acid-conjugated compound | −0.62 | 0.0090 | 1.28 | 0.0207 |
| | 2.88 | 314.1365 | $[M + H]^+$ | feruloyltyramine | −1.02 | 0.0010 | 4.75 | 0.0146 |
| | 2.90 | 312.1227 | $[M + H]^+$ | feruloyltyramine | −0.06 | 0.8772 | 5.54 | 0.0214 |
| | 3.52 | 625.2560 | $[M - H]^-$ | grossamide | ND[d] | ND | 4.26 | 0.0228 |
| | 3.55 | 623.2374 | $[M - H]^-$ | grossamide | ND | ND | 5.42 | 0.0268 |
| 4. secondary metabolites (others) | | | | | | | | |
| | 2.87 | 714.2897 | + | hexose-conjugated compound | −1.47 | 0.0201 | 1.38 | 0.0084 |
| | 2.88 | 805.3345 | + | hexose-conjugated compound | −1.38 | 0.0147 | 1.23 | 0.0138 |
| | 3.00 | 645.2932 | + | fragment ion of $m/z$ 807.3491 | −0.71 | 0.1130 | 1.60 | 0.0074 |
| | 3.01 | 807.3491 | + | hexose-conjugated compound | −0.85 | 0.0826 | 1.52 | 0.0132 |
| | 3.03 | 805.3303 | + | identical with $m/z$ 807.3491 in ESI+ | −0.88 | 0.0521 | 1.28 | 0.0183 |
| | 3.12 | 893.3543 | + | malonylhexose-conjugated compound | −1.22 | 0.1142 | 1.81 | 0.0264 |
| | 3.13 | 891.3327 | + | identical with $m/z$ 893.3543 in ESI+ | −1.24 | 0.0885 | 1.65 | 0.0296 |
| | 5.48 | 497.2361 | $[M + H - 246]^+$ | loroglossin | −2.82 | 0.0017 | −1.16 | 0.0289 |
| | 9.23 | 503.1093 | $[M - H]^+$ | dimer of sulfamethoxazole | 0.65 | 0.1763 | 1.31 | 0.0121 |
| 5. lysophospholipids | | | | | | | | |
| | 4.66 | 593.2735 | $[M - H]^-$ | LysoPI (18:3) | 1.49 | 0.0191 | 1.97 | 0.0237 |
| | 5.12 | 595.2871 | $[M - H]^-$ | LysoPI (18:2) | 2.53 | 0.0322 | 3.93 | 0.0335 |
| | 6.15 | 555.2840 | $[M - H]^-$ | LysoPI (P-16:0) | 1.70 | 0.0172 | 3.47 | 0.0174 |
| | 4.67 | 518.3246 | $[M + H]^+$ | LysoPC (18:3) | 1.89 | 0.0021 | 1.94 | 0.0310 |
| | 4.70 | 562.3159 | $[M + FA - H]^-$ | LysoPC (18:3) | 1.99 | 0.0027 | 1.65 | 0.0144 |
| | 5.00 | 520.3406 | $[M + H]^+$ | LysoPC (18:2) | 2.59 | 0.0041 | 2.27 | 0.0806 |
| | 5.01 | 504.3081 | $[M + FA - 60 - H]^-$ | LysoPC (18:2) | 3.22 | 0.0098 | 2.07 | 0.0392 |
| | 5.01 | 564.3298 | $[M + FA - H]^-$ | LysoPC (18:2) | 2.91 | 0.0056 | 2.21 | 0.0396 |
| | 5.45 | 452.2784 | $[M - H]^-$ | LysoPE (16:0) | 1.60 | 0.0015 | 1.46 | 0.0045 |
| | 5.27 | 431.2206 | $[M - H]^-$ | LysoPA (18:3) | 3.43 | 0.0002 | 4.10 | 0.0083 |
| | 5.88 | 433.2352 | $[M - H]^-$ | LysoPA (18:2) | 2.16 | 0.1109 | 3.56 | 0.0483 |
| | 5.94 | 481.2568 | $[M - H]^-$ | LysoPG (16:1) | 2.38 | 0.0111 | 2.63 | 0.0052 |
| | 6.31 | 483.2720 | $[M - H]^-$ | LysoPG (16:0) | 2.97 | 0.0149 | 1.85 | 0.0431 |
| 6. phospholipids | | | | | | | | |
| | 7.02 | 746.4747 | $[M - H]^-$ | PC (oxo-11:0/18:2) | 0.10 | 0.8652 | −1.46 | 0.0228 |
| | 7.25 | 826.5286 | $[M + H]^+$ | PC (18:3/18:3 + $O_3$) | −0.16 | 0.4734 | −1.30 | 0.0018 |
| | 7.28 | 870.5166 | $[M + FA - H]^-$ | PC (18:3/18:3 + $O_3$) | −0.11 | 0.7091 | −1.31 | 0.0011 |
| | 8.00 | 872.5290 | $[M + FA - H]^-$ | PC (18:2/18:3 + $O_3$) | 0.54 | 0.2351 | −1.25 | 0.0004 |
| | 8.71 | 804.5444 | $[M + H]^+$ | PC (16:0/18:3 + $O_3$) | 0.20 | 0.4386 | −1.08 | 0.0006 |
| | 8.75 | 848.5261 | $[M + FA - H]^-$ | PC (16:0/18:3 + $O_3$) | 0.11 | 0.7257 | −1.63 | 0.0002 |
| | 7.30 | 782.4615 | $[M - H]^-$ | PE (18:3/18:3 + $O_3$) | −0.03 | 0.9326 | −1.13 | 0.0017 |
| | 7.79 | 634.4088 | $[M - H]^-$ | PE (oxo-11:0/16:0) | 0.16 | 0.5829 | −1.01 | 0.0138 |
| | 8.80 | 760.4773 | $[M - H]^-$ | PE (16:0/18:3 + $O_3$) | 0.32 | 0.3440 | −1.02 | 0.0091 |
| 7. free fatty acids | | | | | | | | |
| | 4.58 | 318.2996 | $[M + H]^+$ | phytosphingosine | 0.85 | 0.0002 | 1.24 | 0.0425 |


dx.doi.org/10.1021/jf303702j | J. Agric. Food Chem. 2012, 60, 11015−11028

**Table 2. continued**

| FC | RT (min) | mass ($m/z$) | adduct | tentative identification | 1 h ppi | | 48 h ppi | |
|---|---|---|---|---|---|---|---|---|
| | | | | | $\log_2$[a] | $p$ value[b] | $\log_2$ | $p$ value |
| | 4.89[c] | 293.2100 | $[M - H]^-$ | hydroxylinolenic acid | 2.16 | 0.0595 | 2.34 | 0.0318 |
| | 5.11[c] | 291.1979 | $[M - H]^-$ | ketolinolenic acid | 1.34 | 0.0920 | 1.72 | 0.0361 |
| | 5.26[c] | 295.2268 | $[M - H]^-$ | hydroxylinoleic acid | 1.01 | 0.0334 | 1.32 | 0.0545 |
| | 5.69 | 445.2364 | $[M - H]^-$ | linolenic acid-conjugated lipid | 1.55 | 0.0138 | 2.63 | 0.0257 |
| | 6.56 | 447.2508 | $[M - H]^-$ | linoleic acid-conjugated lipid | 2.22 | 0.0526 | 4.07 | 0.0435 |
| | 6.87[c] | 277.2175 | $[M - H]^-$ | linolenic acid | 1.93 | 0.0096 | 1.40 | 0.0025 |
| | 7.66[c] | 279.2314 | $[M - H]^-$ | linoleic acid | 1.75 | 0.0205 | 1.71 | 0.0049 |
| 8. galactolipids | | | | | | | | |
| | 4.74 | 721.2969 | $[M + FA - H]^-$ | DGMG (18:3) | 0.60 | 0.3714 | −1.82 | 0.0000 |
| | 5.21 | 653.3743 | $[M - H]^-$ | DGMG (16:0) | 1.44 | 0.0102 | 1.57 | 0.0089 |
| | 5.21 | 699.3785 | $[M + FA - H]^-$ | DGMG (16:0) | 1.45 | 0.0148 | 1.52 | 0.0139 |
| | 8.67 | 1069.6010 | $[M - H]^-$ | TGDG (16:3/18:3) | −2.73 | 0.0248 | −2.51 | 0.0220 |
| | 8.67 | 1115.6080 | $[M + FA - H]^-$ | TGDG (16:3/18:3) | −2.74 | 0.0236 | −1.85 | 0.0207 |
| | 9.89 | 797.5392 | $[M + FA - H]^-$ | MGDG (16:0/18:3) | 1.20 | 0.0129 | −1.25 | 0.0304 |

[a]$\log_2$ means $\log_2$[ratio of average peak intensity in pathogen-inoculated samples to that in controls]. [b]$p$ value is calculated by independent two-sample's $t$ test between Ppn -inoculated samples and their corresponding controls. [c]Identification based on accurate mass value and retention time of standantds, +, ESI+ mode, −, ESI- mode. [d]ND, not detected.

to 815.2927 (NL: 32) and 693.2369 (NL: 32 + 122); and ion $m/z$ 891.3327 was fragmented to 847.3120 (NL: 44), 815.2923 (NL: 44 + 32), and 693.2356 (NL: 44 + 32 + 122). The similar MS/MS patterns and retention times of mass ions at $m/z$ 847.3390 ($3.13_{RT}$) and 891.3327 ($3.13_{RT}$) indicated that $m/z$ 847.3390 was most likely a fragment ion of $m/z$ 891.3327. The neutral loss of 122 Da can be a crucial cue for identification of the three unknown compounds in future studies. Furthermore, the occurrence of properties of an identical molecule in both ESI+ and ESI− modes indicated that the molecules at $m/z$ 807.3491 ($3.01_{RT}$) and 893.3543 ($3.12_{RT}$) in ESI+ mode could be identical to those at $m/z$ 805.3303 ($3.03_{RT}$) and $m/z$ 891.3327 ($3.13_{RT}$) in ESI− mode, respectively. In addition, precursor ions of $m/z$ 835.3405 ($2.89_{RT}$) and 921.3427 ($2.98_{RT}$) in ESI− mode showed common neutral losses of 32 and 105 Da. The ion at $m/z$ 835.3405 was fragmented to $m/z$ 803.2886 (NL: 32), 771.2560 (NL: 32 + 32), and 666.2036 (NL: 32 + 32 + 105), and the ion at $m/z$ 921.3427 was fragmented to 877.3176 (NL: 44), 845.3028 (NL: 44 + 32), 813.2665 (NL: 44 + 32 + 32), and 708.2115 (NL: 44 + 32 + 32 + 105). These results indicated that the two compounds at $m/z$ 835.3405 and 921.3427 have the same conjugate, although they have not been identified.

*Identification Based on Lipid Fragmentation Rule.* Phosphatidylcholine (PC) and LysoPC, a type of glycerophospholipids, in ESI+ mode can be fragmented to $m/z$ 184 $[C_5H_{15}NO_4P]^+$, 125 $[C_2H_6O_4P]^+$, and 86 $[C_5H_{12}N]^+$ as shown in Figure 4A,C.[39,40] The fragment ions were observed in the MS/MS spectra of molecular ions at $m/z$ 518.3246 ($4.67_{RT}$), 520.3406 ($5.00_{RT}$), 826.5286 ($7.25_{RT}$), and 804.5444 ($8.71_{RT}$), thereby indicating that the molecules were PCs or LysoPCs (Table 1; Supporting Information, Supplementary Figures 1−18, 19, 23, and 25). Furthermore, on the basis of an integrative interpretation of the literature on similar compounds,[41] metabolome databases, and molecules identified in ESI− mode, LysoPC (18:3) at $m/z$ 518.3246, LysoPC (18:2) at $m/z$ 520.3406, trioxidized PC (16:0/18:3 + $O_3$) at $m/z$ 804.5444, and trioxidized PC (18:3/18:3 + $O_3$) at $m/z$ 826.5286 were tentatively identified. In addition, the MS/MS pattern of the $m/z$ 318.2996 ion showed a neutral loss of 54 (18 + 18 + 18) Da for $3H_2O$, indicating that the molecule contained three hydroxyl groups (Table 1; Supporting Information, Supplementary Figures 1−16). Together with the metabolome database-based results, the molecule was identified as phytosphingosine.

In ESI− mode, all phospholipids were commonly fragmented to $m/z$ 171 $[GP - H]^-$, 153 $[GP - H_2O - H]^-$, and 79 $[PO_3]^-$ (Figure 4B). Specific daughter ions at $m/z$ 241 for PI and LysoPI (Figure 4B) as well as at $m/z$ 245 for PG and LysoPG (Supporting Information, Supplementary Figures 2−35 and 37) were released. Furthermore, in ESI− mode, the MS/MS spectra of phospholipids and galactosyl lipids generated carboxylate anions $[RCOO^-]$ of *sn*-1 and *sn*-2 fatty acids with a neutral loss of fatty acids [RCOOH] or [RCOOH − $H_2O$]. A neutral loss of 60 Da is generated in the MS/MS spectra of formic acid (FA)-adducted LysoPC and PC.[34,42] For example, Figure 4B shows that a molecular ion at $m/z$ 593.2735 was fragmented to $m/z$ 277.21 $[18:3 - H]^-$, 241.01 $[C_6H_{11}O_8P - H]^-$, 223.00 $[C_6H_{11}O_8P - H - H_2O]^-$, 171.00 $[GP - H]^-$, 152.99 $[GP - H_2O - H]^-$, and 78.96 $[PO_3]^-$ with a neutral loss of 278.21 Da [18:3], thereby indicating that the molecule was a PI class with linolenic acid [18:3]. Finally, with reference to metabolome databases, the molecular ion at $m/z$ 593.2735 was identified as LysoPI (18:3). Moreover, a molecular ion at $m/z$ 870.5166 was fragmented to $m/z$ 824.47 (NL of 46 Da for FA), 810.48 (NL of 60 Da indicating FA-adducted LysoPC or PC), 502.27 (NL of 60 + 308.19 for $[18:3 + O_3 - H_2O]$), 325.19 $[18:3 + O_3 - H]^-$, 293.18 [NL of $O_2$ from (linolenic acid + $O_3$ − H)$^-$], and 277.20 $[18:3 - H]^-$ as shown in Figure 4D. The MS/MS spectra showed the neutral losses of 46 and 60 Da indicating FA-adducted LysoPC or PC. Furthermore, a neutral loss of $[18:3 + O_3 - H_2O]$ and fragment ions of $[18:3 + O_3 - H]^-$ and $[18:3 - H]^-$ indicated that the molecule was trioxidized at either the *sn*-1 or *sn*-2 positioned fatty acid in PC and PC(18:3/18:3 + $O_3$). On the basis of the mentioned fragmentation rules of lipids, the relevant literature on similar compounds, and metabolome databases, the phospholipids and galactosyl lipids were identified (Supporting Information, Supplementary Figure 2).

**Quantitative Changes of Metabolites by Compatible Plant−Pathogen Interaction.** ROS have known to be involved in a protective system in plants against pathogen

attack by activating signaling pathways for defense responses, oxidative cross-linking of cell walls, and acting as an antimicrobial agent.[9] Moreover, ROS play a role in successful pathogenesis by destroying host membrane lipids, thereby facilitating the penetration of pathogens.[43,44] In the present study, quantitative changes of several types of amino acids, secondary metabolites, and lipids were detected at the first (1 h ppi) and second (48 h ppi) phases of the ROS burst after inoculation of compatible pathogen, *Ppn* (Table 2).

**Changes of Amino Acids and Secondary Metabolites.** Differential accumulation of phenylpropanoids including feruloylquinic acid, ferulic acid, quinic acid, and cafeoylquinic acid was observed compared to those in the corresponding control. The biosynthesis of the phenylpropanoids is mediated by phenylalanine ammonia-lyase (PAL), which converts L-phenylalanine to *trans*-cinnamic acid in the first step of the phenylpropanoid pathway. In the present experiment, with the increase of feruloylquinic acid and its intermediates (ferulic acid and quinic acid), a slight but statistically significant decrease of phenylalanine was observed at 1 h ppi (Table 2), suggesting that the PAL-mediated reaction could be activated at the first ROS burst in *Ppn*-inoculated tobacco. Indeed, the positive correlation between the up-regulation of PAL activity and $H_2O_2$ has been demonstrated in *Arabidopsis* and tomato.[45,46] Phenolic compounds derived from the PAL-mediated pathway contribute to the defense system acting as potent inhibitors of oxidative stress and as peroxide scavengers cooperating with peroxidase.[47] These phenolic compounds also function in cell wall lignification, which is one of the major immune responses to pathogen, as subunits of lignin.[48] In addition, the increase of feruloylquinic acid and the decrease of caffeoylquinic acid at 1 h ppi suggest the activation of caffeic acid *O*-methyltransferase, which methylates caffeic acid to ferulic acid and/or caffeoylquinic acid to feruloylquinic acid. Caffeic acid *O*-methyltransferase-suppressed tobacco also has enhanced susceptibility as compared to the control,[49,50] indicating that the methylation of caffeic acid to ferulic acid may lead to critical impacts on lignin composition for enhanced pathogen resistance.

At 48 h ppi, three phenolic amino acids, tryptophan-derived compounds (indole-3-carboxaldehyde and tryptamine), and hydroxycinnamic acid amides (HCAAs) conjugated with tyrosine- and phenylalanine-derived compounds were increased. HCAAs, including feruloyltyramine (FT) and a FT dimer (grossamide), as well as indole-3-carboxaldehyde and tryptamine contribute to the plant defense against pathogen through their peroxidative incorporation into the cell wall to form covalent cross-linked polymers and through their activity as antibiotic agents.[51−53] In pepper, two HCAAs, FT and coumaoyltyramine (CT), are dramatically induced at HR appearance during incompatible interactions followed by declining bacterial growth (*Xanthomonas campestris* pv. *campestris* and *Xanthomonas axonopodis* pv. *vesicatoria*/*avrBs1*), but only weak traces of the HCAAs emerge during compatible interactions followed by substantial growth (*X. axonopodis* pv. *vesicatoria*).[54] When lipopolysaccharides, which induce defense responses in plants, are pretreated before inoculation of compatible pathogen in pepper plants, the synthesis of FT and CT is also considerably activated with enhanced resistance to pathogen,[54] indicating that the accumulation of these compounds contributes to the resistance of plant to pathogen. In *Arabidopsis*, the accumulation of tryptophan-derived compounds, such as indole-3-carboxaldehyde, reaches much higher levels in incompatible interactions than in compatible interactions.[53]

As described above, the changes in the accumulation of amino acids, HCCAs, phenylpropanoids, and indolic metabolites induced by compatible tobacco-*Ppn* interaction were similar to the responses that have been reported in incompatible plant−pathogen interactions. These results may reflect the host responses attempting to block pathogen penetration, and their degree of change may be an important factor to determine compatibility to the pathogen.

**Changes of Lipid Composition.** Table 2 shows that lysophospholipids were significantly increased by >2-fold at 1 and 48 h ppi. Lysophospholipid is produced by hydrolysis of a fatty acid at either the *sn*-1 or -2 position of a phospholipid by phospholipase A (PLA).[55] The PLA-mediated lysophospholipid accumulation is most likely accompanied by release of the free fatty acid. Indeed, linolenic acid and linoleic acid were increased at 1 and 48 h ppi (Table 2). Accumulated evidence has shown that the pathogen (elicitor)-induced oxidative burst is linked with a PLA-mediated defense pathway.[55,56] For example, an elicitor-induced oxidative burst is accompanied by PLA activation, and the inhibition of PLA activity results in suppression of the oxidative burst in soybean cells.[56] LysoPC, a product of PLA, has the following effects: activation of a tonoplast H+/Na+ antiporter; induction of a transient shift of intracellular and apoplastic pH levels; and activation of several signal transductions, including $Ca^{2+}$ influx.[57]

Lipid peroxidation of membrane phospholipids occurs in response to oxidative stress, and it is one of the major outcomes of free radical-mediated injury to tissue.[58] In the present study, the decrease of oxidized phospholipids was observed at 48 h ppi. The quantitative change of oxidized phospholipids was reversely correlated with that of lysophospholipids, thereby suggesting that oxidized fatty acids in phospholipids could be preferentially hydrolyzed to lysophospholipids. The concomitant increase of ketolinolenic acid and hydroxylinolenic acid implied this possibility. The oxidation of phospholipids preferentially occurs at the *sn*-2 positioned fatty acid rather than at the *sn*-1 positioned fatty acid.[58] The oxidized fatty acid at the *sn*-2 position of phospholipids is hydrolyzed by phospholipase $A_2$ and is then converted into oxylipins, which are involved in plant defense responses.[49,58] The preferential removal of oxidized fatty acid from oxidized phospholipids may reflect the metabolite rearrangement to acclimate or overcome cell damages occurring in *Ppn*-inoculated tobacco.

In addition, phytosphingosine was increased at 1 and 48 h ppi (Table 2). Sphingolipids have been suggested to act in the cellular signaling of stress responses and programmed cell death through the regulation of the ROS production.[59] Accumulation of phytosphingosine was observed in *Arabidopsis* leaves infected with a HR-inducing *Pseudomonas syringae*.[60] The induction of cell death by sphingoid bases including phytosphingosine is suppressed by the treatment of phosphorylated sphingoid bases in *Arabidopsis*, suggesting that the relative ratio between phosphorylated and unphosphorylated sphingoid bases is a crucial determinant of cell fate toward proliferation or death.[59,61] Altogether, the increase of phytosphingosine in the present study suggested the involvement of phytosphingosine in the production of ROS followed by cell death in this compatible pathogen inoculated tobacco.

Glycoglycerolipids are most abundant in the photosynthetic membrane (thylakoid) in plants.[62,63] The quantitative changes in glycoglycerolipids by *Ppn* inoculation indicated composi-

tional and/or structural changes of the chloroplast membrane at 1 and 48 h ppi (Table 2). In particular, the increase of DGMG (16:0) and the decrease of DGMG (18:3) and MGDG (16:0/18:3) at 48 h ppi suggested that the preferential hydrolysis of linolenic acid at either the *sn*-1 or *sn*-2 position of glycoglycerolipids could occur.

In summary, using nontargeted metabolite profiling in *Ppn*-inoculated tobacco (*N. tabacum* L. cv. Wisconsin 38) and multivariate statistical analyses (PCA and OPLS-DA), non-redundant 355 and 345 pathogen-responsive candidate mass ions were selected in ESI+ and ESI− mode, respectively. Finally, 76 mass ions were identified on the basis of their accurate mass ions and MS/MS spectra. Phenolic amino acids, phenylpropanoids, hydroxycinnamic acid amides, oxidized linolenic acids, free fatty acids, lysophospholipids, glycoglycerolipids, and trioxidized phospholipids were identified as changed after *Ppn* inoculation. These compounds have been implicated in defense responses to biotic and abiotic stresses. The identification of the defense-related compounds in nontargeted metabolite profiled using UPLC-MS indicated that the metabolomics approach is a powerful tool to investigate metabolic responses of plant−pathogen interactions. However, of 76 mass ions with MS/MS spectra, 39 ions could not be completely identified due to insufficient data from the metabolome databases based on LC-MS. Additional metabolome databases will provide more opportunities for investigating novel molecules implicated in plant defense.

## ■ ASSOCIATED CONTENT

### Ⓢ Supporting Information

Identification of 28 and 48 pathogen-responsive mass ions on the basis of their MS/MS spectra in positive and negative modes, respectively. Normalized peak intensities of non-redundant Ppn-responsive mass ions (335 and 345 ions) in ESI+ and ESI−, respectively, at 1 and 48 h post pathogen inoculation. This material is available free of charge via the Internet at http://pubs.acs.org.

## ■ AUTHOR INFORMATION

### Corresponding Author

*Phone: 82-2-6943-4132. Fax: 82-2-6943-4109. E-mail: nammh@kbsi.re.kr.

### Funding

This work was supported by Grant T32602 from the Korea Basic Science Institute to M.H.N. and PJ008045 from the Next-Generation BioGreen 21 Program of the Rural Development Administration, Republic of Korea.

### Notes

The authors declare no competing financial interest.

## ■ ACKNOWLEDGMENTS

We gratefully acknowledge Seong Hwa Park for her technical support.

## ■ ABBREVIATIONS USED

DGMG, digalactosylmonoacylglycerol; CT, coumaoyltyramine; FA, formic acid; FT, feruloyltyramine; HCAA, hydroxycinnamic acid amide; HR, hypersensitive response; MGDG, monogalactosyldiacylglycerol; NL, neutral loss; PAL, phenylalanine ammonia-lyase; PC, phosphatidylcholine; PI, phosphatidylinositol; PLA, phospholipase A; *Ppn*, *Phytophthora parasitica* var. *nicotianae*; ROS, reactive oxygen species; TGDG, trigalactosyldiacylglycerol.

## ■ REFERENCES

(1) Bari, R.; Jones, J. D. Role of plant hormones in plant defence responses. *Plant Mol. Biol.* **2009**, *69* (4), 473−488.

(2) Li, A.; Wang, X.; Leseberg, C. H.; Jia, J.; Mao, L. Biotic and abiotic stress responses through calcium-dependent protein kinase (CDPK) signaling in wheat (*Triticum aestivum* L.). *Plant Signal. Behav.* **2008**, *3* (9), 654−656.

(3) Bruce, T. J.; Pickett, J. A. Plant defence signalling induced by biotic attacks. *Curr. Opin. Plant Biol.* **2007**, *10* (4), 387−392.

(4) Peng, J. Y.; Huang, Y. P. The signaling pathways of plant defense response and their interaction. *Zhi Wu Sheng Li Yu Fen Zi Sheng Wu Xue Xue Bao* **2005**, *31* (4), 347−353.

(5) Jaspers, P.; Kangasjarvi, J. Reactive oxygen species in abiotic stress signaling. *Physiol. Plant.* **2010**, *138* (4), 405−413.

(6) Torres, M. A. ROS in biotic interactions. *Physiol. Plant.* **2011**, *138* (4), 414−429.

(7) Mittler, R.; Vanderauwera, S.; Suzuki, N.; Miller, G.; Tognetti, V. B.; Vandepoele, K.; Gollery, M.; Shulaev, V.; Van Breusegem, F. ROS signaling: the new wave? *Trends Plant Sci.* **2011**, *16* (6), 300−309.

(8) Suzuki, N.; Koussevitzky, S.; Mittler, R.; Miller, G. ROS and redox signalling in the response of plants to abiotic stress. *Plant Cell Environ.* **2012**, *35* (2), 259−270.

(9) Shetty, N. P.; Jørgensen, H. J. L.; Jensen, J. D.; Collinge, D. B.; Shetty, H. S. Roles of reactive oxygen species in interactions between plants and pathogens. *Eur. J. Plant Pathol.* **2008**, *121*, 267−289.

(10) Kobayashi, M.; Ohura, I.; Kawakita, K.; Yokota, N.; Fujiwara, M.; Shimamoto, K.; Doke, N.; Yoshioka, H. Calcium-dependent protein kinases regulate the production of reactive oxygen species by potato NADPH oxidase. *Plant Cell* **2007**, *19* (3), 1065−1080.

(11) Yoshioka, H.; Sugie, K.; Park, H. J.; Maeda, H.; Tsuda, N.; Kawakita, K.; Doke, N. Induction of plant gp91 phox homolog by fungal cell wall, arachidonic acid, and salicylic acid in potato. *Mol. Plant−Microbe Interact.* **2001**, *14* (6), 725−736.

(12) Wi, S. J.; Ji, N. R.; Park, K. Y. Synergistic biosynthesis of biphasic ethylene and reactive oxygen species in response to hemibiotrophic *Phytophthora parasitica* in tobacco plants. *Plant Physiol.* **2012**, *159* (1), 251−265.

(13) Heller, J.; Tudzynski, P. Reactive oxygen species in phytopathogenic fungi: signaling, development, and disease. *Annu. Rev. Phytopathol.* **2011**, *49*, 369−390.

(14) Torres, M. A.; Jones, J. D.; Dangl, J. L. Reactive oxygen species signaling in response to pathogens. *Plant Physiol.* **2006**, *141* (2), 373−378.

(15) De Vos, R. C.; Moco, S.; Lommen, A.; Keurentjes, J. J.; Bino, R. J.; Hall, R. D. Untargeted large-scale plant metabolomics using liquid chromatography coupled to mass spectrometry. *Nat. Protoc.* **2007**, *2* (4), 778−791.

(16) Maruyama, K.; Takeda, M.; Kidokoro, S.; Yamada, K.; Sakuma, Y.; Urano, K.; Fujita, M.; Yoshiwara, K.; Matsukura, S.; Morishita, Y.; Sasaki, R.; Suzuki, H.; Saito, K.; Shibata, D.; Shinozaki, K.; Yamaguchi-Shinozaki, K. Metabolic pathways involved in cold acclimation identified by integrated analysis of metabolites and transcripts regulated by DREB1A and DREB2A. *Plant Physiol.* **2009**, *150* (4), 1972−1980.

(17) Urano, K.; Maruyama, K.; Ogata, Y.; Morishita, Y.; Takeda, M.; Sakurai, N.; Suzuki, H.; Saito, K.; Shibata, D.; Kobayashi, M.; Yamaguchi-Shinozaki, K.; Shinozaki, K. Characterization of the ABA-regulated global responses to dehydration in *Arabidopsis* by metabolomics. *Plant J.* **2009**, *57* (6), 1065−1078.

(18) Lehmann, M.; Schwarzlander, M.; Obata, T.; Sirikantaramas, S.; Burow, M.; Olsen, C. E.; Tohge, T.; Fricker, M. D.; Moller, B. L.; Fernie, A. R.; Sweetlove, L. J.; Laxa, M. The metabolic response of *Arabidopsis* roots to oxidative stress is distinct from that of heterotrophic cells in culture and highlights a complex relationship between the levels of transcripts, metabolites, and flux. *Mol. Plant* **2009**, *2* (3), 390−406.

(19) Sanchez, D. H.; Siahpoosh, M. R.; Roessner, U.; Udvardi, M.; Kopka, J. Plant metabolomics reveals conserved and divergent metabolic responses to salinity. *Physiol. Plant.* **2008**, *132* (2), 209−219.
(20) Cho, K.; Shibato, J.; Agrawal, G. K.; Jung, Y. H.; Kubo, A.; Jwa, N. S.; Tamogami, S.; Satoh, K.; Kikuchi, S.; Higashi, T.; Kimura, S.; Saji, H.; Tanaka, Y.; Iwahashi, H.; Masuo, Y.; Rakwal, R. Integrated transcriptomics, proteomics, and metabolomics analyses to survey ozone responses in the leaves of rice seedling. *J. Proteome Res.* **2008**, *7* (7), 2980−2998.
(21) Kim, J. K.; Bamba, T.; Harada, K.; Fukusaki, E.; Kobayashi, A. Time-course metabolic profiling in *Arabidopsis thaliana* cell cultures after salt stress treatment. *J. Exp. Bot.* **2007**, *58* (3), 415−424.
(22) Shulaev, V.; Cortes, D.; Miller, G.; Mittler, R. Metabolomics for plant stress response. *Physiol. Plant.* **2008**, *132* (2), 199−208.
(23) t'Kindt, R.; Morreel, K.; Deforce, D.; Boerjan, W.; Van Bocxlaer, J. Joint GC-MS and LC-MS platforms for comprehensive plant metabolomics: repeatability and sample pre-treatment. *J. Chromatogr., B: Anal. Technol. Biomed. Life Sci.* **2009**, *877* (29), 3572−3580.
(24) Schripsema, J. Application of NMR in plant metabolomics: techniques, problems and prospects. *Phytochem. Anal.* **2010**, *21* (1), 14−21.
(25) Arbona, V.; Iglesias, D. J.; Talon, M.; Gomez-Cadenas, A. Plant phenotype demarcation using nontargeted LC-MS and GC-MS metabolite profiling. *J. Agric. Food Chem.* **2009**, *57* (16), 7338−7347.
(26) von Roepenack-Lahaye, E.; Degenkolb, T.; Zerjeski, M.; Franz, M.; Roth, U.; Wessjohann, L.; Schmidt, J.; Scheel, D.; Clemens, S. Profiling of *Arabidopsis* secondary metabolites by capillary liquid chromatography coupled to electrospray ionization quadrupole time-of-flight mass spectrometry. *Plant Physiol.* **2004**, *134* (2), 548−559.
(27) Horai, H.; Arita, M.; Kanaya, S.; Nihei, Y.; Ikeda, T.; Suwa, K.; Ojima, Y.; Tanaka, K.; Tanaka, S.; Aoshima, K.; Oda, Y.; Kakazu, Y.; Kusano, M.; Tohge, T.; Matsuda, F.; Sawada, Y.; Hirai, M. Y.; Nakanishi, H.; Ikeda, K.; Akimoto, N.; Maoka, T.; Takahashi, H.; Ara, T.; Sakurai, N.; Suzuki, H.; Shibata, D.; Neumann, S.; Iida, T.; Funatsu, K.; Matsuura, F.; Soga, T.; Taguchi, R.; Saito, K.; Nishioka, T. MassBank: a public repository for sharing mass spectral data for life sciences. *J. Mass Spectrom.* **2010**, *45* (7), 703−714.
(28) Ivanova, P. T.; Milne, S. B.; Myers, D. S.; Brown, H. A. Lipidomics: a mass spectrometry based systems level analysis of cellular lipids. *Curr. Opin. Chem. Biol.* **2009**, *13* (5−6), 526−531.
(29) Matsuda, F.; Yonekura-Sakakibara, K.; Niida, R.; Kuromori, T.; Shinozaki, K.; Saito, K. MS/MS spectral tag-based annotation of non-targeted profile of plant secondary metabolites. *Plant J.* **2009**, *57* (3), 555−577.
(30) Lin, L. Z.; Harnly, J. M. A screening method for the identification of glycosylated flavonoids and other phenolic compounds using a standard analytical approach for all plant materials. *J. Agric. Food Chem.* **2007**, *55* (4), 1084−1096.
(31) Cuyckens, F.; Claeys, M. Mass spectrometry in the structural analysis of flavonoids. *J. Mass Spectrom.* **2004**, *39* (1), 1−15.
(32) Hanhineva, K.; Rogachev, I.; Kokko, H.; Mintz-Oron, S.; Venger, I.; Karenlampi, S.; Aharoni, A. Non-targeted analysis of spatial metabolite composition in strawberry (*Fragaria* × *ananassa*) flowers. *Phytochemistry* **2008**, *69* (13), 2463−2481.
(33) Gomez-Romero, M.; Segura-Carretero, A.; Fernandez-Gutierrez, A. Metabolite profiling and quantification of phenolic compounds in methanol extracts of tomato fruit. *Phytochemistry* **2010**, *71* (16), 1848−1864.
(34) O'Donnell, V. B. Mass spectrometry analysis of oxidized phosphatidylcholine and phosphatidylethanolamine. *Biochim. Biophys. Acta* **2011**, *1811* (11), 818−826.
(35) Ivanova, P. T.; Milne, S. B.; Byrne, M. O.; Xiang, Y.; Brown, H. A. Glycerophospholipid identification and quantitation by electrospray ionization mass spectrometry. *Methods Enzymol.* **2007**, *432*, 21−57.
(36) Seca, A. M.; Silva, A. M.; Silvestre, A. J.; Cavaleiro, J. A.; Domingues, F. M.; Pascoal-Neto, C. Lignanamides and other phenolic constituents from the bark of kenaf (*Hibiscus cannabinus*). *Phytochemistry* **2001**, *58* (8), 1219−1223.
(37) Dauwe, R.; Morreel, K.; Goeminne, G.; Gielen, B.; Rohde, A.; Van Beeumen, J.; Ralph, J.; Boudet, A. M.; Kopka, J.; Rochange, S. F.; Halpin, C.; Messens, E.; Boerjan, W. Molecular phenotyping of lignin-modified tobacco reveals associated changes in cell-wall metabolism, primary metabolism, stress metabolism and photorespiration. *Plant J.* **2007**, *52* (2), 263−285.
(38) Guo, B. *Transformation of Sulfonamide Antibiotics on Soil Mineral Oxides*. M.S. thesis, Graduate School of Clemson University, 2008; http://gradeworks.umi.com//14/62/1462205.html.
(39) Liebisch, G.; Scherer, M. Quantification of bioactive sphingo- and glycerophospholipid species by electrospray ionization tandem mass spectrometry in blood. *J. Chromatogr., B: Anal. Technol. Biomed. Life Sci.* **2011**, *883*−*884*, 141−146.
(40) Liebisch, G.; Schmitz, G. Quantification of lysophosphatidylcholine species by high-throughput electrospray ionization tandem mass spectrometry (ESI-MS/MS). *Methods Mol. Biol.* **2009**, *580*, 29−37.
(41) Adachi, J.; Asano, M.; Yoshioka, N.; Nushida, H.; Ueno, Y. Analysis of phosphatidylcholine oxidation products in human plasma using quadrupole time-of-flight mass spectrometry. *Kobe J. Med. Sci.* **2006**, *52* (5), 127−140.
(42) Xia, Y. Q.; Jemal, M. Phospholipids in liquid chromatography/mass spectrometry bioanalysis: comparison of three tandem mass spectrometric techniques for monitoring plasma phospholipids, the effect of mobile phase composition on phospholipids elution and the association of phospholipids with matrix effects. *Rapid Commun. Mass Spectrom.* **2009**, *23* (14), 2125−2138.
(43) Able, A. J. Role of reactive oxygen species in the response of barley to necrotrophic pathogens. *Protoplasma* **2003**, *221* (1−2), 137−143.
(44) Temme, N.; Tudzynski, P. Does *Botrytis cinerea* ignore $H_2O_2$-induced oxidative stress during infection? Characterization of *Botrytis* activator protein 1. *Mol. Plant−Microbe Interact.* **2009**, *22* (8), 987−998.
(45) Desikan, R.; Reynolds, A.; Hancock, J. T.; Neill, S. J. Harpin and hydrogen peroxide both initiate programmed cell death but have differential effects on defence gene expression in *Arabidopsis* suspension cultures. *Biochem. J.* **1998**, *330* (Part 1), 115−120.
(46) Gayoso, C.; Pomar, F.; Novo-Uzal, E.; Merino, F.; de Ilarduya, O. M. The Ve-mediated resistance response of the tomato to *Verticillium dahliae* involves $H_2O_2$, peroxidase and lignins and drives PAL gene expression. *BMC Plant Biol.* **2010**, *10*, 232.
(47) Ali, M. B.; Yu, K. W.; Hahn, E. J.; Paek, K. Y. Methyl jasmonate and salicylic acid elicitation induces ginsenosides accumulation, enzymatic and non-enzymatic antioxidant in suspension culture *Panax ginseng* roots in bioreactors. *Plant Cell Rep.* **2006**, *25* (6), 613−620.
(48) Vogt, T. Phenylpropanoid biosynthesis. *Mol. Plant* **2010**, *3* (1), 2−20.
(49) La Camera, S.; Gouzerh, G.; Dhondt, S.; Hoffmann, L.; Fritig, B.; Legrand, M.; Heitz, T. Metabolic reprogramming in plant innate immunity: the contributions of phenylpropanoid and oxylipin pathways. *Immunol. Rev.* **2004**, *198*, 267−284.
(50) Pincon, G.; Maury, S.; Hoffmann, L.; Geoffroy, P.; Lapierre, C.; Pollet, B.; Legrand, M. Repression of *O*-methyltransferase genes in transgenic tobacco affects lignin synthesis and plant growth. *Phytochemistry* **2001**, *57* (7), 1167−1176.
(51) Facchini, P. J.; Hagel, J.; Zulak, K. G. Hydroxycinnamic acid amide metabolism: physiology and biochemistry. *Can. J. Bot.* **2002**, *80* (6), 577−589.
(52) Hagel, J. M.; Facchini, P. J. Elevated tyrosine decarboxylase and tyramine hydroxycinnamoyltransferase levels increase wound-induced tyramine-derived hydroxycinnamic acid amide accumulation in transgenic tobacco leaves. *Planta* **2005**, *221* (6), 904−914.
(53) Hagemeier, J.; Schneider, B.; Oldham, N. J.; Hahlbrock, K. Accumulation of soluble and wall-bound indolic metabolites in *Arabidopsis thaliana* leaves infected with virulent or avirulent *Pseudomonas syringae* pathovar tomato strains. *Proc. Natl. Acad. Sci. U.S.A.* **2001**, *98* (2), 753−758.

(54) Newman, M. A.; von Roepenack-Lahaye, E.; Parr, A.; Daniels, M. J.; Dow, J. M. Prior exposure to lipopolysaccharide potentiates expression of plant defenses in response to bacteria. *Plant J.: Cell Mol. Biol.* **2002**, *29* (4), 487−495.
(55) Chapman, K. D. Phospholipase activity during plant growth and development and in response to environmental stress. *Trends Plant Sci.* **1998**, *3* (11), 419.
(56) Chandra, S.; Heinstein, P. F.; Low, P. S. Activation of phospholipase A by plant defense elicitors. *Plant Physiol.* **1996**, *110* (3), 979−986.
(57) Viehweger, K.; Dordschbal, B.; Roos, W. Elicitor-activated phospholipase A(2) generates lysophosphatidylcholines that mobilize the vacuolar H(+) pool for pH signaling via the activation of Na(+)-dependent proton fluxes. *Plant Cell* **2002**, *14* (7), 1509−1525.
(58) Catala, A. Lipid peroxidation of membrane phospholipids generates hydroxy-alkenals and oxidized phospholipids active in physiological and/or pathological conditions. *Chem. Phys. Lipids* **2009**, *157* (1), 1−11.
(59) Shi, L.; Bielawski, J.; Mu, J.; Dong, H.; Teng, C.; Zhang, J.; Yang, X.; Tomishige, N.; Hanada, K.; Hannun, Y. A.; Zuo, J. Involvement of sphingoid bases in mediating reactive oxygen intermediate production and programmed cell death in *Arabidopsis*. *Cell Res.* **2007**, *17* (12), 1030−1040.
(60) Peer, M.; Stegmann, M.; Mueller, M. J.; Waller, F. Pseudomonas syringae infection triggers de novo synthesis of phytosphingosine from sphinganine in *Arabidopsis thaliana*. *FEBS Lett.* **2010**, *584* (18), 4053−4056.
(61) Hait, N. C.; Oskeritzian, C. A.; Paugh, S. W.; Milstien, S.; Spiegel, S. Sphingosine kinases, sphingosine 1-phosphate, apoptosis and diseases. *Biochim. Biophys. Acta* **2006**, *1758* (12), 2016−2026.
(62) Murata, N. H. S.; Fujimura, Y. Glycerolipids in various preparations of photosystem II from spinach chloroplasts. *Biochim. Biophys. Acta* **1990**, *1019*, 261−268.
(63) Block, M. A.; Jouhet, J.; Maréchal, E.; Bastien, O.; Joyard, J. Role of the envelope membranes in chloroplast glycerolipid biosynthesis. In *Advances in Photosynthesis and Respiration. Vol. 34: Photosynthesis*; Eaton-Rye, J. J., Tripathy, B. C., Sharkey, T. D., Eds.; Springer Netherlands: Dordrecht, The Netherlands, 2012; pp 191−216